2015

Forest Fire Risk Assessment Using Point Process Modeling & Monte Carlo Fire Simulation: A Case Study in Gyeongju, South Korea

Hyeyoung Woo
University of Montana - Missoula

FOREST FIRE RISK ASSESSMENT USING POINT PROCESS MODELING & MONTE CARLO FIRE SIMULATION: A CASE STUDY IN GYEONGJU, SOUTH KOREA

By

HYEYOUNG WOO

B.S., Seoul National University, Seoul, Korea, 2007

Thesis

presented in partial fulfillment of the requirements
for the degree of

Master of Science in Forestry

The University of Montana
Missoula, MT

May 2015

Approved by:

Sandy Ross, Dean of The Graduate School
Graduate School

Woodam Chung, Chair
College of Forestry and Conservation

Carl Seielstad,
College of Forestry and Conservation

Jonathan Graham,
Department of Mathematical Sciences

Woo, Hyeyoung, Master of Science, May 2015 *Forestry*

Forest Fire Risk Assessment Using Point Process Modeling & Monte Carlo Fire Simulation: A Case Study in Gyeongju, South Korea

Chairperson: Woodam Chung

Forest fire risk assessment becomes critical for developing forest and fire management strategies in Korea since the magnitude of damage from fires significantly increased over the past decades. Fire behavior probability is one of the major components in quantifying fire risk, and is often presented as burn probability. Burn probability estimation requires a proper estimation of fire occurrence probability because fire spread is largely influenced by ignition locations in addition to other environmental factors, such as weather, topography, and land covers.

The objective of this study is to assess forest fire risk over a large forested landscape in and around the City of Gyeongju, Republic of Korea, while incorporating fire occurrence probability into estimation of burn probability. A fire occurrence probability model with spatial covariates and autocorrelation was developed using historical record of fire occurrence between 1991 and 2012 and a spatial point processing (SPP) method. A total of 502 fire ignition points were generated using the fire occurrence probability model. Monte Carlo fire spread simulations were performed from the ignition points under the 95% extreme weather scenario, resulting in burn probability estimation for each land parcel across the landscape. Finally, the burn probability was combined with government-appraised land property value to assess potential loss value per land parcel due to forest fires.

The density of forest fires of the study landscape was associated with lower elevation, moderate slope, coniferous land cover, distance to road, and higher tomb density. A positive spatial autocorrelations between the locations of fire ignition was also found. An area-interaction point process model including the spatial covariate effects and interpoint interaction term appeared to be suitable as a fire occurrence probability model. A correlation analysis among the fire occurrence probability, burn probability, land property value, and potential value loss indicates that fire risk is largely associated with spatial pattern of burn probability (Pearson's correlation r=0.7084). These results can provide forest and fire management authorities in the study region with useful information for decision making. It is also hoped that the methodology presented here can provide an improved framework for assessing fire risk in other regions.

ACKNOWLEDGEMENTS

I am deeply grateful to my supervisor Dr. Woodam Chung for his encouragement and providing me with all the support for carrying out the study. I would also like to thank my graduate committee members Dr. Carl Seielstad and Dr. Jon Graham for their valuable guidance. I appreciate Dr. Byungdoo Lee and Korea Forest Research Institute sharing the opportunity and data for the research. I also thank Lucas Wells who provided technical assistance and insights, and Kate Clyatt who helped proofread and grammar-check. A special thanks to my family; Dr. Woongsoon Jang, my husband, and my children, Youngjun and Sophie, for their patience and support throughout the process of completing this thesis.

LIST OF CONTENTS

Page

LIST OF TABLES

Table Page

LIST OF FIGURES

Figure Page

CHAPTER 1

Overview

Increased potential risk of forest fires has been one of the main concerns in forest management. Real and visible threats of fires often attract public attention on the need to assess and address fire hazard in forested lands especially near urban, suburban, rural and agricultural lands. A long tradition of fire suppression and prevention lead to the excessive accumulation of flammable fuels in many landscapes around the world, partly causing larger and more severe fires. This "wildfire paradox" calls for a strategic fire risk assessment (Calkin et al., 2014), which includes clear objectives and integrated approaches in understanding physical, ecological and social aspects of fire (McCaffrey et al., 2013).

The process of forest fire risk assessment generally includes the estimation of potential loss and probability of the loss taking place (McCaffrey, 2006). Finney (2005) and Tutsch et al. (2010) presented these two components as fire effect and fire behavior probability, respectively. Fire behavior probability is often measured as burn probability, the number of times a unit area burned against the total number of burning. It is important to distinguish burn probability from fire occurrence probability which indicates the relative frequency of fires, even though they are often used interchangeably. Fire occurrence probability does not involve a likelihood of fire spread, thus provides limited sight of fire risk assessment. On the other hand, burn probability cannot be evaluated adequately without involving an estimation of fire occurrence probability, because fires are not randomly ignited. The occurrence of fire is influenced by numerous environmental factors such as topography, fuels, and human accessibility while the spread of fire is influenced by weather, topography, and fuels. Previous research efforts were mostly put into assessing forest fire risks either based on fire occurrence probability as a surrogate for fire behavior probability, or by analyzing fire behavior probability without adequately incorporating fire occurrence probability.

Relying on only one measure in fire risk assessment certainly limits our ability to fully understand potential fire risks (Finney, 2005; Bar Massada et al., 2009).

The goal of this study is to provide a consolidated insight into forest fire risk assessment by integrating fire occurrence probability, burn probability and social values of a given study landscape. This study is anticipated to serve the needs of constructing a more accurate and comprehensive fire-risk map (Carmel et al., 2008) which would help in forest planning and decision-making on resource allocation for fire management. This study consists of two major parts: 1) construction of a forest fire ignition density model for a given study landscape, and 2) estimation of burn probability in each land parcel across the landscape. The city of Gyeongju located in Gyeongsangbuk-do, Republic of Korea (Korea) was used as a study landscape because of its abundant fire records over the past 20 years. The two major parts of the study are presented in detail in Chapters 1 and 2, respectively.

A spatial point processing (SPP) was used to develop a forest fire ignition density model that estimates the likelihood of fire occurrence based on fire history and local characteristics of the study landscape. Topography, land cover, and the accessibility to public transportation and community infrastructure (e.g. roads and structures) for the study landscape were selected as the variables influencing the fire occurrence probability. A large number of fire ignition locations were derived from the density model and used to simulate fire spreads across the landscape. The areas burned from each simulated fire during a given fire duration were recorded and used to estimate burn probability in each 10m x 10m pixel on the landscape. A forest fire spread model developed by Lee et al. (2011) was used as a fire simulator. Burn probability was then combined with government-appraised property value of each pixel on the study landscape to estimate potential loss.

The density of forest fire ignition points in Gyeongju was found to be associated with lower elevation, lower slope, coniferous land cover, distance to road, and higher tomb density. An indication of additional clustering of ignition points was observed after taking into account the spatial trends. Thus, an inhomogeneous area-interaction point process model with both the spatial covariates effect and a positive interpoint interaction term was developed to estimate the likelihood of fire occurrence over the study landscape. The resulted point process model exhibited better goodness of fit and performance compared to an inhomogeneous Poisson point process model and a spatial logistic regression model.

A total of 502 fire ignition points were generated using the fire occurrence probability model for Monte Carlo fire spread simulation. Burn probability calculated per pixel ranged from 0.0 to 0.076, and revealed forest lands around Geumo and Gumi mountains as high burn probability areas. Potential loss estimated as a product of burn probability and government-appraised land property value ranged approximately between 0 and 19,000 won per m^2. The results showed that the potential loss was more affected by burn probability (Pearson's correlation $r = 0.7084, p < 0.0001$) than property value.

This study demonstrates that it is practically feasible to estimate burn probability using Monte Carlo fire spread simulation while incorporating fire occurrence probability. It is hoped that the fire risk assessment approach developed in this study, as well as the end product of the study, a spatial distribution of fire risk represented by potential loss, can provide useful information for forest and fire management planning across a large landscape.

Chapter 1. Modeling forest fire ignition pattern in Gyeongju, Korea

1.1 Introduction

Predicting the occurrences of forest fire has long been examined with a variety of different methodologies. Frequently, analyses involve investigations of spatial patterns of fire occurrences as a consequence of several spatial covariates (e.g., topography, weather and human activities) or physical properties of fire (e.g., propagation and spotting). With advanced geographical information systems (GIS) and spatial statistical analysis tools, recent studies have been attempting to respond to needs for accurate prediction of natural or human caused fire occurrences.

There are several factors that generally influence forest fire ignition, including elevation, weather, fuel characteristics, and accessibility to public transportation and community facilities (such as roads, buildings, and campsites). These natural and human environmental factors have been commonly analyzed as variables in past studies on fire occurrence (e.g., Chou et al., 1993; Vega-García et al., 1993; Pew et al., 2001; Preisler et al., 2004). However, their influences on fire occurrence may vary vastly across ecosystems, both spatially and temporally (Yang et al., 2007), Therefore, distinctive site-specific features should be identified for different regions and accounted for as environmental variables that affect fire occurrence. In Portugal, where agriculture residue burning is a common practice, agricultural land use was found to be a significant predictor of fire ignition (Catry et al., 2010). Conversely, density of goats and sheep was linked to fire ignition in a region of central Spain (Romero-Calcerrada et al., 2008). Mercer and Prestemon (2005) linked socio-economic variables such as poverty and unemployment with occurrence of wildfires. Police density or whether it is Saturday or not were considered as potential predictos of arson-caused wildfires in Florida (Prestemon and Butry, 2005). Likewise, many previous studies agree that

cultural characteristics and behaviors should also be considered to derive appropriate explanatory variables for forest fire ignition.

In Korea, most forest fires are anthropogenic. No naturally occurring forest fire was reported in Korea during the recent 3 decades (Lee et al., 2006). Korea is a mountainous country with almost 70% of its territory being forested. The country is unique in that there are many fragmented croplands and a large number of tombs located on forestlands. Both of these characteristics are closely related with forest fire events in Korea. According to the annual report of forest fire statistics (Korea Forest Service, 2012), an average of 387 forest fires burned 733.77 hectares across the entire territory of Korea annually from 2002 to 2011. The major causes of these forest fires were campers and hikers (44%), followed by incineration of garbage (8%), agricultural residues (7%), and tomb visitors (7%). Although tomb visitors accounted for only 7% of the total forest fire occurrence in these statistics, its proportion could be larger because 4% of forest fires in Korea started with improperly discarded cigarettes, likely from hikers and tomb visitors. Thus, densities of tombs and croplands as well as roads or hiking trails could potentially be related to the occurrence of forest fires in Korea.

Environmental, developmental, and cultural attributes of the region may thereby be associated with each other and collectively influence the fire occurrences. Conventionally, previous studies have adopted a logistic regression modeling approach involving these factors for spatially estimating forest fire probability (Prestemon et al., 2013) (e.g., Pew et al., 2001; Garcia et al., 1995; Catry et al., 2010; Preisler et al., 2004; Chou, 1993), since the occurrence of fire can be regarded as binary (i.e. presence-absence). The method postulates a finite number of randomly selected absence points (or pixels) to compare them with cases of presence. However, Pearce and Boyce (2006) noted that most geographical distribution data are actually presence-only data rather

than presence-absence, and warned that logistic regression models might not be appropriate in most instances because of this "pseudo-absence" problem. The term pseudo-absence indicates that randomly generated absence points of an event do not necessarily represent true absence and may thus introduce bias in prediction. Warton and Shepherd (2010) later encouraged the use of spatial point processes (SPP) for the construction of "specificationally, interpretatively, and implementationally sound" modeling, and proved the asymptotic equivalence of logistic regression to Poisson point process modeling.

The main idea of an SPP is to consider the locations of objects of interest (e.g. trees, cells, animals, etc.) as points, and derive inferences about the pattern of those points with or without parameters (Illian et al., 2008). The pattern refers to the configuration of a set of finite points in a multidimensional (usually two) space. The points may be randomly distributed across the plane, clustered, or dispersed. The parameters influence the spatial arrangement of points and may incorporate spatial trends of auxiliary variables, spatial dependence of the response variable itself (i.e. spatial autocorrelation), or both. The advance of computational techniques and statistical tools have promoted the use of SPP in analyzing spatial data with complicated covariates using different model-based and simulation-based approaches. Various extensions of SPP models are available, including homogeneous or inhomogeneous Poisson, Gibbs, Cox, and marked point process models, which have been widely used to explain natural or artificial events such as species distribution patterns in forestry (Stoyan and Penttinen, 2000).

In terms of analyzing the patterns of forest fires, Podur et al. (2003) initiated the application of spatial point pattern analysis to occurrences of lightning-caused forest fires in Ontario, Canada, finding that locations of fires are clustered at a relatively small scale, but regularly spaced at a larger scale. Genton et al. (2006) and Hering et al. (2009) demonstrated useful implementations of

extensions of the K-function (e.g., L-function, inhomogeneous K- and K-cross function) on cause-specific wildfire ignition locations in a region of Florida. Turner (2009) also employed the use of point process modelling techniques in analysis of forest fire location data. Yang et al. (2007) examined the influence of several spatial covariates involving topography, ownership, and municipalities on human-caused forest fires in the Missouri Ozark highlands and developed a point process model of fire occurrence probability under an assumption of a heterogeneous spatial trend.

These previous studies successfully contributed to the introduction of the SPP to forest fire analysis. However, their application is limited by either a narrow focus on statistical properties of forest fires or, exclusive of social and ecological perspectives, does not fully utilize the statistical information available. For example, the occurrence of spatial dependence among the response variables themselves (especially at small scales), often referred to as spatial autocorrelation, has been widely used in interpreting ecological data. However, only a few existing studies have adequately addressed this aspect of forest fire occurrence (e.g., Chou et al., 1993; Hering et al., 2009; Juan et al., 2012).

In this study, we aimed to model the density of forest fire ignitions using SPP while taking advantage of both statistical and environmental information available. Environmental factors affecting the occurrence of forest fire, as well as the interactions between fire occurrences were considered simultaneously in the forms of spatial covariates and autocorrelations, respectively, in order to derive more accurate predictions of fire probability. To address these objectives, we examined forest fire ignition data from 1991 to 2012 over a study landscape in Korea. The locations of forest fire ignition during the past 21 years were recorded as a point pattern and analyzed based on the theory of SPP. The fundamentals of this theory will be expanded upon in the next section. Using factors such as topography (elevation, aspect, and slope), land use, forest

type, and human accessibility (distance to road and structures), the density of fire ignition points was modeled and the influence of each variable on forest fire occurrence addressed. The densities of tombs and croplands were also considered in the model as variables to take into account any site-specific and cultural characteristics. Spatial autocorrelation of ignition locations was examined in order to verify the attributes of the forest fire ignition point pattern at both small- and large-scales. To account for all these factors, three possible models were suggested in phases: 1) homogeneous Poisson model (null model, involving neither spatial trends nor autocorrelation), 2) inhomogeneous Poisson model (spatial trends without autocorrelation), and 3) inhomogeneous area-interaction model (spatial trends with autocorrelation). We compared the performances of the three models with different structures, as well as the conventional logistic regression model, and chose the best model based on AIC to obtain a more reliable prediction for forest fire ignition probability in the study landscape. The estimation of fire ignition density provided by the final model is expected to be useful for further investigation of forest fire risk assessment for the study region.

1.2 Spatial Point Process Modeling

Spatial point process (SPP) modeling is the most common method for analyzing spatial point process data. The collection of locations, x_i $(i = 1, \dots, n)$, representing an object or event of interest (e.g. forest fire ignition location) forms a point pattern $\mathbf{x} = \{x_1, \dots, x_n\}$ in a bounded region. Usually a point location x_i is denoted as an event in order to distinguish it from an arbitrary point location $\boldsymbol{u}$ (Diggle, 1983).

The goal of a SPP model is to elucidate and model the spatial structure of event locations in a stochastic manner. The structure of a set of finite point locations (i.e. point pattern) is

categorized by its first- and second- order spatial structure. The first-order property is the intensity of the process, λ, which denotes the density of events per unit area. The intensity λ at any point $\boldsymbol{u}$ in the region is represented as:

$$\lambda(\boldsymbol{u}) = \lim_{|d\boldsymbol{u}|\to 0}\left\{\frac{\mathrm{E}(n(d\boldsymbol{u}))}{|d\boldsymbol{u}|}\right\}, \quad (1)$$

where $d(\boldsymbol{u})$ denotes a small region around the point $\boldsymbol{u}$, $n(du)$ is the number of events in $d(\boldsymbol{u})$, $\mathrm{E}(n(d\boldsymbol{u}))$ is the expected number of events in $d(\boldsymbol{u})$ and $|d\boldsymbol{u}|$ is the area of $d(\boldsymbol{u})$. The intensity of a point pattern can be either constant or variable over the domain. Intensity given as a function of location allows for environmental conditions to vary by location, resulting in spatial trend (Law et al., 2009).

The second-order property represents the variability in the relative frequency of pairs of events. In other words, it measures how the location of one event u_i is related to another event u_j either positively (i.e. attraction) or negatively (i.e. inhibition), and is defined as:

$$\gamma(u_i, u_j) = \lim_{du_i, du_j\to 0}\left\{\frac{\mathrm{E}(n(du_i)n(du_j))}{|du_i||du_j|}\right\}. \quad (2)$$

Again du_i and du_j denote infinitesimal areas around the points u_i and u_j respectively ($i \neq j$). Under an assumption of stationarity, this function depends only on the difference between u_i and u_j in distance and direction, not on their absolute locations; thus, this second-order property is described as the covariance (or correlation) between the points.

A point pattern is one realization of a process regulated by the mixture of the first-order and the second-order properties. That is, the probability that an event is found at a given location is determined conditionally by the effect of spatial covariates (i.e. spatial trends), the relative position to the other events (i.e. covariance/correlation structure), or both. The intensity of such a

process will vary conditionally as a function of location $\boldsymbol{u}$ and the configuration of the point pattern **x**. This is called the Papangelou conditional intensity (Papangelou, 1974) $\lambda(\boldsymbol{u}, \mathbf{x})$, specified as;

$$\lambda(\boldsymbol{u}, \mathbf{x}) = b(\boldsymbol{u}) \prod_{i=1}^{n(\mathbf{x})} c(\boldsymbol{u}, x_i) \tag{3}$$

where $b(\boldsymbol{u})$ denotes the spatial covariate effects and $\prod_{i=1}^{n(\mathrm{x})} c(\boldsymbol{u}, x_i)$ refers to the product of interactions between point $\boldsymbol{u}$ and every event x_i in the process **x** where $\boldsymbol{u} \neq x_i$. The equation can then be written in a log-linear form and parameterized by $= (\theta_1, \theta_2)$ as:

$$\log\lambda_\theta(u, \mathrm{x}) = \theta_1 B(u) + \theta_2 C(u, \mathrm{x}) \tag{4}$$

such that the set of parameters θ can be estimated. For Poisson processes, maximum likelihood is used to estimate parameters (Berman and Turner, 1992), and for other exponential families of distributions maximum pseudolikelihood is used (Baddeley and Turner, 2000, extended by Besag et al., 1982). The resulting intensity is viewed as the probability density function of the event over the area. With a proper sampling procedure, point patterns can be simulated from the density function estimated by Eq. (4). An application of the probability density function and simulation from this function will be described in the next chapter.

1.2.1 Homogeneous Poisson Processes and Complete Spatial Randomness

When the first order intensity of a process is constant over the region (i.e. $\lambda(u) = \lambda$ in Eq (1)) and the locations of events are independent of each other (i.e. $\gamma(u_i, u_j) = \lambda^2$ for any pairs of locations u_i and u_j in Eq. (2)), the point pattern is equivalent to a set of points with randomly generated x- and y- coordinates from a uniform distribution. Under this setting, the numbers of events in a region with area $|A|$ are Poisson distributed with mean $\lambda|A|$. This is the simplest type of spatial point pattern, termed a homogeneous Poisson point process. A homogeneous Poisson point process is said to exhibit complete spatial randomness (CSR) which often serves as the null

hypothesis in a point pattern analysis. Other more complicated point processes such as Cox (Cox and Isham, 1980), Markov models (Van Lieshout, 2000), and space-time point processes (Ogata, 1998) are deemed generalizations of the homogeneous Poisson process.

1.2.2 Inhomogeneous Poisson Process

The assumption of invariant intensity across the region, known as stationarity, is not usually satisfied in real applications. Most natural and social phenomena are closely related to spatial locations of other covariates. For example, incidence of disease may be associated with a factory pollutant (Lloyd et al., 1985), and locations of animals are likely to be affected by locations of predators or competing species (Stein and Georgiadis, 2006). Therefore, the probability an event occurs at a given location may fluctuate over a given region according to some spatial covariates. The conditional intensity in this case is $\lambda(\boldsymbol{u}, \mathbf{x}) = \lambda(\boldsymbol{u})$, instead of $\lambda(\boldsymbol{u}, \mathbf{x}) = \lambda$ (as in the homogeneous Poisson process). Note that this still retains independence between the occurrences of events. A point process with such attributes is characterized as an inhomogeneous Poisson process.

Consider a set of points representing the locations of trees scattered over an area. When a finite number of trees is randomly distributed within the region, they exhibit CSR and are assumed to arise from a homogeneous planar Poisson process (Figure 1a). However, if there is variation in moisture content associated with proximity to a river, trees are more likely to be situated in the vicinity of the river (Figure 1b). The probability density function here may be based on the Euclidean distance to the river, and the pattern of trees is regarded as one realization of an inhomogeneous Poisson process. Consequently, a cluster of trees appears near the river. The conditional density of the inhomogeneous Poisson process is estimated as $\log\lambda_\theta(\boldsymbol{u}, \mathbf{x}) = \theta_1 B(\boldsymbol{u})$ in Eq. (4) where $B(\boldsymbol{u})$ denotes the Euclidean distance of location $\boldsymbol{u}$ to the river. Note that the

locations of points are still independent in this process. In other words, there is no interaction between the locations of trees (i.e. $C(\boldsymbol{u}, \mathbf{x})$ is set to 0 in Eq. (4)). Therefore, some clustering or dispersion among the points may be present in an inhomogeneous Poisson process purely as a consequence of a particular spatial covariate.

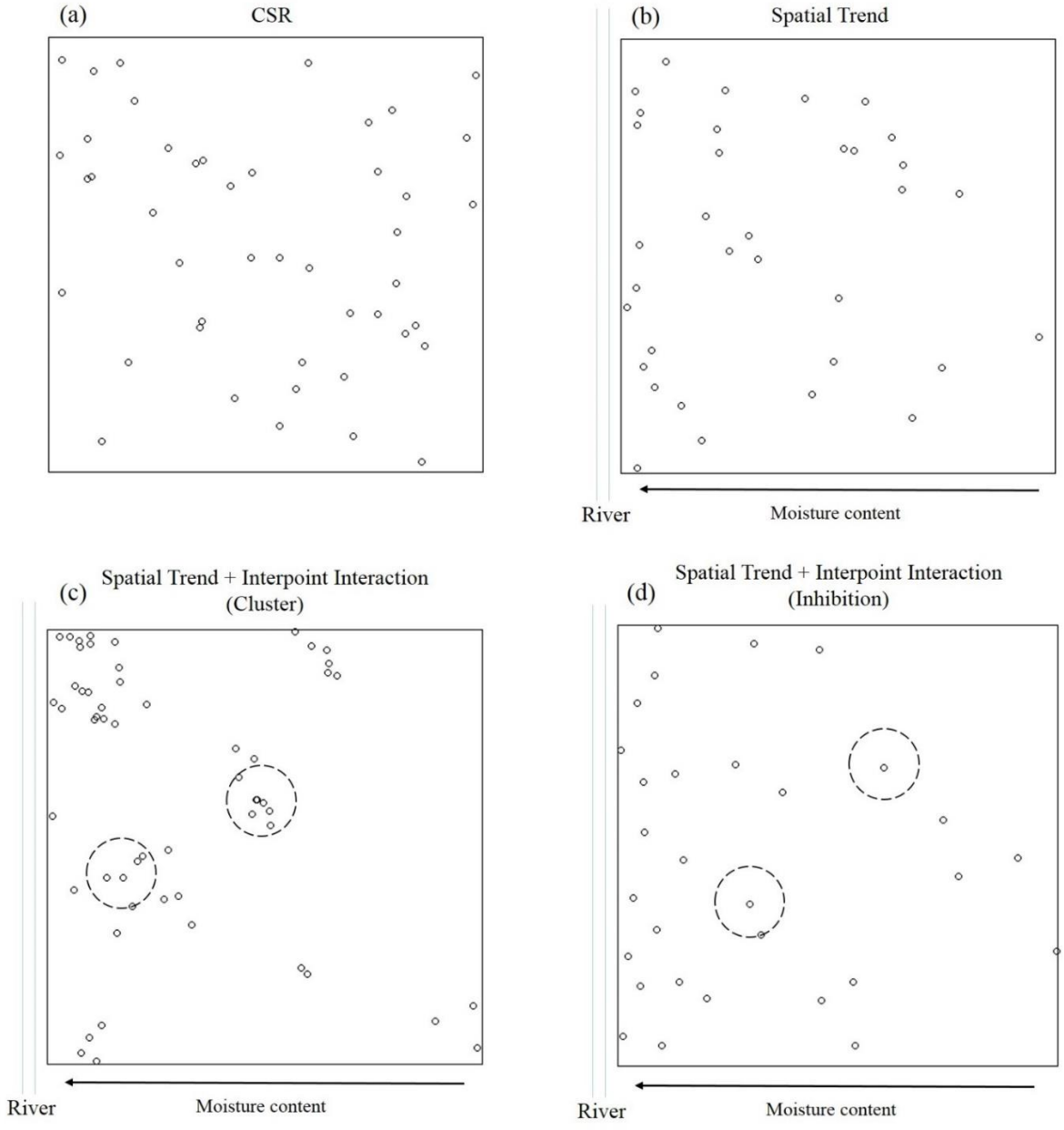

Figure 1.1. (a) Point patterns reflecting the effects of complete spatial randomness, (b) spatial trend of moisture content as a function of Euclidean distance to river, (c) spatial trend with attractive interpoint interaction, and (d) spatial trend with inhibitory interpoint interaction.

1.2.3 Markov Point Process: Area-Interaction Process

It often becomes difficult to interpret patterns of points using only the effect of covariate spatial trends, especially when there appears to be excessive aggregation or regularity among the events. For instance, a situation may arise in which points naturally cluster themselves (e.g. due to short-distance dispersal of seeds from a plant) (Figure 1d), or inhibit one another (e.g. due to canopy cover for shade intolerant species) (Figure 1c). The location of one event is no longer independent of the locations of other events, especially of neighbors. Spatial trends can also be incorporated into a model for the interaction among the events, though it may be difficult to separate the two sources of spatial structure in practice.

Markov models are types of point process models that deal with dependence among events as a pairwise interaction within the extent of a pre-defined neighborhood. The term "Markov property" indicates that an event is influenced only by nearby events. Markov processes thus postulate a range of influence for neighbors to exert an effect, usually within a disc of a certain radius r centered at the point in two dimensions. The Papangelou conditional intensity for Markov models is the product of spatial trend and interaction expressed as Eq. (3) where $c(\boldsymbol{u}, x_i)$ is the pairwise interaction function. Generally $c(\boldsymbol{u}, x_i) = c(x_i, \boldsymbol{u})$ (i.e. symmetric pairwise interaction) and $c(\boldsymbol{u}, x_i)$ depends only on the distance between $\boldsymbol{u}$ and x_i, not their actual locations. The interaction function $c(\boldsymbol{u}, x_i)$ is defined differently in different Markov models. For example, in the Strauss model, a prototype of the Markov point process model suggested by Strauss (1975), the function is expressed as:

$$t(\boldsymbol{u}, \mathrm{x}) = \#\{x_i \in \mathbf{x} : \|\boldsymbol{u} - x_i\| \leq r\} \qquad (5)$$

such that interacting events are no more than r units apart. Writing $\prod_{i=1}^{n(\mathbf{x})} c(\boldsymbol{u}, x_i)$ as $\gamma^{t(\boldsymbol{u},\mathbf{x})}$ and $b(\boldsymbol{u})$ as β for constant parameters β & γ in Eq. (3), the conditional intensity for the Strauss model is simplified as

$$\lambda(\boldsymbol{u}, \mathbf{x}) = \beta\gamma^{t(\boldsymbol{u},\mathbf{x})}. \tag{6}$$

The resulting probability density function for a univariate Strauss point process is expressed as:

$$f(\mathbf{x}) = \begin{cases} \alpha\beta^{n(\mathbf{x})}\gamma^{s(\mathbf{x})} \; if \; \gamma > 0 \\ \alpha\beta^{n(\mathbf{x})} \; if \; \gamma = 0 \end{cases} \tag{7}$$

where $n(\mathbf{x})$ is the number of points in a point pattern $\mathbf{x}$ and $s(\mathbf{x})$ is the number of pairs of points within the range of r in $\mathbf{x}$. The parameter β represents the first order intensity, γ represents the direction and magnitude of interaction, and α is a normalizing constant. When $\gamma = 0$ the process exhibits extreme inhibition (i.e. hard core process). When $0 < \gamma < 1$ the points exhibit repulsion and when $\gamma > 1$ the points exhibit attraction. If γ equals to 1, the Strauss process is a Poisson process.

Kelly and Ripley (1976), however, noted that the Strauss function is not integrable for parameter values $\gamma > 1$ and is thus inappropriate for a clustered pattern. An alternative called an area-interaction point process was introduced by Baddeley and Van Lieshout (1995). The fundamental difference between the area-interaction process and the Markov models is that the area-interaction function is based on the area of a neighborhood (i.e. influence zone) rather than the Euclidean distance of each pair of points. The general form of the density function in an area-interaction process is specified as

$$f(\mathbf{x}) = \alpha\beta^{n(\mathbf{x})}\gamma^{-|U(\mathbf{x},r)|} \tag{8}$$

where $|U(\mathbf{x}, r)|$ denotes the area of the union of discs of radius r centered at x_i such that $x_i \in \mathbf{x}$. Mathematically $|U(\mathbf{x}, r)|$ is expressed as

$$|U(\mathbf{x}, r)| = \bigcup_{i=1}^{n} B(x_i, r) \tag{9}$$

where $B(x_i, r) = \{a \in \Re^2 : \|a - x_i\| \leq r\}$ (i.e. a disc of radius r centered at event x_i).

The conditional intensity at an event x_i of an area-interaction process is

$$\lambda(x_i, \mathbf{x}) = \beta \gamma^{-B(x_i, r) \setminus |U(\mathbf{x}, r)|}. \tag{10}$$

The area described here (the exponent of γ in Eq. (10)) represents the area of the disc with radius r centered on an event x_i, which is not covered by the other discs centered at x_j where $i \neq j$ in a point pattern $\mathbf{x}$. In other words, it indicates the area further added by event x_i to the existing area of the union of discs centered at x_j. For a fixed radius r, if the points are clustered together, the sum of $B(x_i, r) \setminus |U(\mathrm{x}, r)|$ will be small and the overlapping area will be larger, causing the term γ to be greater than 1. If the points are spatially dispersed, the sum of single occupancy by each event will be maximized while the multiple occupancy would be minimized, so the term γ is expected to be smaller than 1. When $\gamma = 1$ it is equivalent to the Poisson process, which has no interaction, similar to the Strauss process. Unlike the Strauss model, however, the area-interaction model is known to be stable and well-defined for all values of γ, producing stable models for both clustered and dispersed point patterns.

Baddeley and Van Lieshout (1995) asserted that the area-interaction process may be a reasonable model to explain many biological phenomena such as territorial exclusion by individual animals or a herd of prey running away from predators. Despite drawbacks such as the ambiguity of interpretation for parameter γ in practical applications, use of area-interaction process models

and their extensions appear widely (e.g. Picard et al. 2009; Juan et al. 2012; Uria-Diez et al. 2013) due to their stability and flexibility in dealing with natural patterns of features.

1.2.4 Summary Statistics and Model Diagnosis

1.2.4.1 Ripley's K- (L-) function

An analysis for a SPP typically starts by investigating to what extent a given point pattern departs from a null hypothesis of CSR (i.e. homogeneous Poisson process). Useful graphical summary statistics for examining the nature of point patterns are available, such as a smoothed kernel density for the first-order global intensity, or the $\hat{G}$- and $\hat{F}$-functions for the second-order property (Diggle, 1983). Ripley's K-function (Ripley, 1977) is the most widely used tool for examining both the first- and second- order properties of a homogeneous SPP simultaneously. The idea of the K-function is to calculate the average number of events within a radius r of a randomly chosen event. Letting this radius r vary, the K-function is specified as a function of r as:

$$K(r) = \lambda_0^{-1} E[\#\text{ of events within distance } r \text{ of a randomly chosen event}]$$

where λ_0 is the mean number of events per unit area. Under the null hypothesis of CSR the expected number of events within a distance r from each event is theoretically equivalent to the area of a circle of radius r (πr^2), yielding $K(r) = \pi r^2$. If there is clustering of events, the observed number of neighbors is likely to be larger than the mean number of events per unit area (i.e. $K(r) > \pi r^2$). If the events are regularly spaced, on the other hand, fewer neighbors will appear (i.e. $K(r) < \pi r^2$) especially at short distances. The Ripley's L-function (Besag, 1977; Ripley, 1991) is a transformation of the K-function which normalizes $K(r)$ to $L(r) = \sqrt{K(r)/\pi} - r$. The L-function converges to 0 when the null hypothesis is satisfied; $L(r) > 0$ indicates clustering while $L(r) < 0$ indicates regularity.

Although the hypothesis of CSR provides a basic understanding of point pattern, most natural and human phenomena are not expected to be completely homogeneous throughout space. Clustering of events is usually due to underlying environmental heterogeneity, as seen in the example of Figure 1b (clustering of tree locations in areas with higher moisture content). Thus, we may instead be concerned with clustering (or inhibition) over and above the underlying spatial trends or interaction, rather than against CSR. The inhomogeneous K- (L-) function enables detection of departure from a non-stationary point process such as an inhomogeneous Poisson (or inhomogeneous Markov) model. This K-function is intensity-reweighted in relation to the location of an event and its neighboring events, and again involves second-order summary characteristics. The inhomogeneous K-function is thus defined as:

$$K_{inhom}(r) = \frac{1}{|A|} E\left(\sum_{x_i \in \mathrm{x} \cap \mathrm{A}} \sum_{x_j \in \mathrm{x} \setminus \{x_i\}} \frac{I(\|x_i - x_j\| \le r)}{\lambda(x_i)\lambda(x_j)} \right)$$

where $|A|$ denotes the area of a bounded Borel set within which the points are distributed and x_i and x_j denote any pair of events with $i \neq j$ in point pattern **x**. The right-hand side of the equation represents the mean number of points within a disc of radius r from each point with a second-order property (see Eq. (2)). The local intensities (i.e. $\lambda(x_i)$ and $\lambda(x_j)$) are estimated nonparametrically (e.g. using a kernel smoothed density) around each point rather than using the constant λ. The normalized inhomogeneous L-function is analogously defined as: $L_{inhom}(r) = \sqrt{K_{inhom}(r)/\pi} - r$.

Assessing whether a given point pattern departs from a null hypothesis (whether stationary or non-stationary) is achieved by constructing the extrema of empirical K-functions (typically 95% confidence bands) obtained through Monte Carlo random sampling. We can also use the K-function with a hypothesized point process model to examine goodness-of-fit for SPP models

(Stoyan and Penttinen, 2000). Inhomogeneous K-function supports, in particular, an inspection of interpoint interactions after allowing for spatial trends of a point pattern (Baddeley et al., 2000).

1.2.4.2 Residual Analysis: Four-panel Plot and Residual Q-Q Plot

Baddeley et al. (2004) proposed techniques for conducting a residual analysis for spatial point process models which are analogous to those for classical regression models. The four-panel residual plot provides integrated presentation of diagnostic plots for both spatial trends and residuals. The plot contains panels with a marked plot, a contour plot of the smoothed residual field and a lurking variable plot for the location coordinates. The marked plot displays the intensity λ which is constant or conditionally varying over the region, with a greyscale map with circles whose radius is proportional to the residual mass. The contoured image plot shows a smoothed kernel density of the residuals accounting for an edge effect. The smoothed residual field at a location $\boldsymbol{u}$ will be approximately 0 if the model is correctly fitted. The lurking variable plot depicts the cumulative residuals as a function of the x & y coordinates and uses confidence envelopes to assess whether the model requires inclusion of any particular variables, or the process exhibits heterogeneity. These plots facilitate investigation of quality of fit for the fitted model and effects of spatial covariates, and provide a visual way of evaluating the goodness-of-fit of the model.

The four-panel plot, however, is only for assessing spatial trends and is inappropriate for detecting the effect of interaction between events. Baddeley et al. (2004) devised a diagnostic tool for interpoint interaction using properties of the joint distribution of the residuals in a generalized linear model. This procedure compares the empirical quantiles of the smoothed residual field values to the expected quantiles obtained by Monte Carlo simulations of a given point process model, giving a type of Q-Q plot. If the model specifies the interpoint interaction correctly, the

point-wise residual quantiles of the simulated model will be equivalent to that of the original point pattern and will approximately depict a 45-degree line.

1.2.4.3 Model Selection

The Akaike information criterion (AIC) (Akaike, 1974) is one of the most widely used model selection tools, valued for its inferential and restrictive competence (Bozdogan, 1987). It is defined as

$$\text{AIC} = -2\max(\text{log-likelihood}) + 2 * (\text{number of parameters})$$

where the 2nd term in the sum represents a penalty on the number of model parameters. Generally, models with smaller AIC values provide a better fit for the data. AIC can also be used to choose the best model among several proposed models, as long as their log-likelihoods are tractable.

1.3 Application of SPP to model the density of forest fire ignitions

In this study, we examined the past forest fire ignition locations recorded for 21 years (1991 ~ 2011) in Gyeongju, South Korea to develop a fire ignition density model using an SPP. We first hypothesized that the intensity of forest fire ignition points (i.e. first-order property) exhibits spatial trend over the region. The null model was a homogeneous Poisson process. The kernel smoothed density and the estimated L-function for the point pattern of forest fire ignition locations were calculated with 200 iterations of Monte Carlo simulation to examine whether or not there was a departure from CSR, and if there was, whether the departure approached clustering or regularity.

Subsequently, we explored the use of several spatial covariates (e.g. topography, land cover, and human accessibility within the study area) likely to affect the density of forest fire ignition points. The ignitions of forest fires are expected to occur more frequently in areas with

lower elevation, gentle slopes, and south facing aspects, as these topographical attributes are related to higher population density. Proximity to public transportation and community infrastructures such as roads and buildings are also associated with higher density of forest fires, due to greater accessibility by humans. Additionally, the density of tombs and croplands were incorporated into this model because of their unique cultural characteristics and historic role in fire ignition. The species composition of forest stands may also be relevant to the occurrence of forest fires, since pine dominated stands are more likely to catch fire from resin characteristics (Bradley et al., 1992). Among these possible spatial covariates, significant predictors of intensity for forest fire ignition points were selected through the use of numerical & graphical tools such as AIC and lurking variable plots resulting from an inhomogeneous Poisson process model fit.

After modeling the density of the point pattern using the spatial covariates, the goodness-of-fit of the model was evaluated by estimating the inhomogeneous L-function and conducting a residual analysis with multiple simulations. The null model in this case was an inhomogeneous Poisson process including only the selected covariates, not any interpoint interaction. However, if there was any evidence indicating that the local intensity of the ignition points was not fully explained by incorporation of spatial trends – particularly that there was potential for interaction between the points – an inhomogeneous area-interaction process could be considered as an alternative. Estimation of the inhomogeneous L-function and construction of the four-panel plot and residual Q-Q plot were also considered for the area-interaction model to verify model performance.

Among the three different models (homogeneous Poisson, inhomogeneous Poisson, and inhomogeneous area-interaction model), a final model was chosen which exhibited the most adequate fit based on the diagnostic plots and which presented the smallest AIC value.

Furthermore, the AIC of a spatial logistic regression model for the same dataset was included to highlight the value of SPP models against the classic lattice-based models for predicting density of forest fire ignition locations. The map displaying the spatial distribution of modeled fire density and the corresponding realization of fire locations was developed as the end product of this study. This map is used for further investigation related to fire spread in the next chapter. All the spatial analysis and modelling procedures were implemented using the R package "spatstat" (Baddeley and Turner, 2004). The overall flow of the analysis procedure is shown in Figure 2.

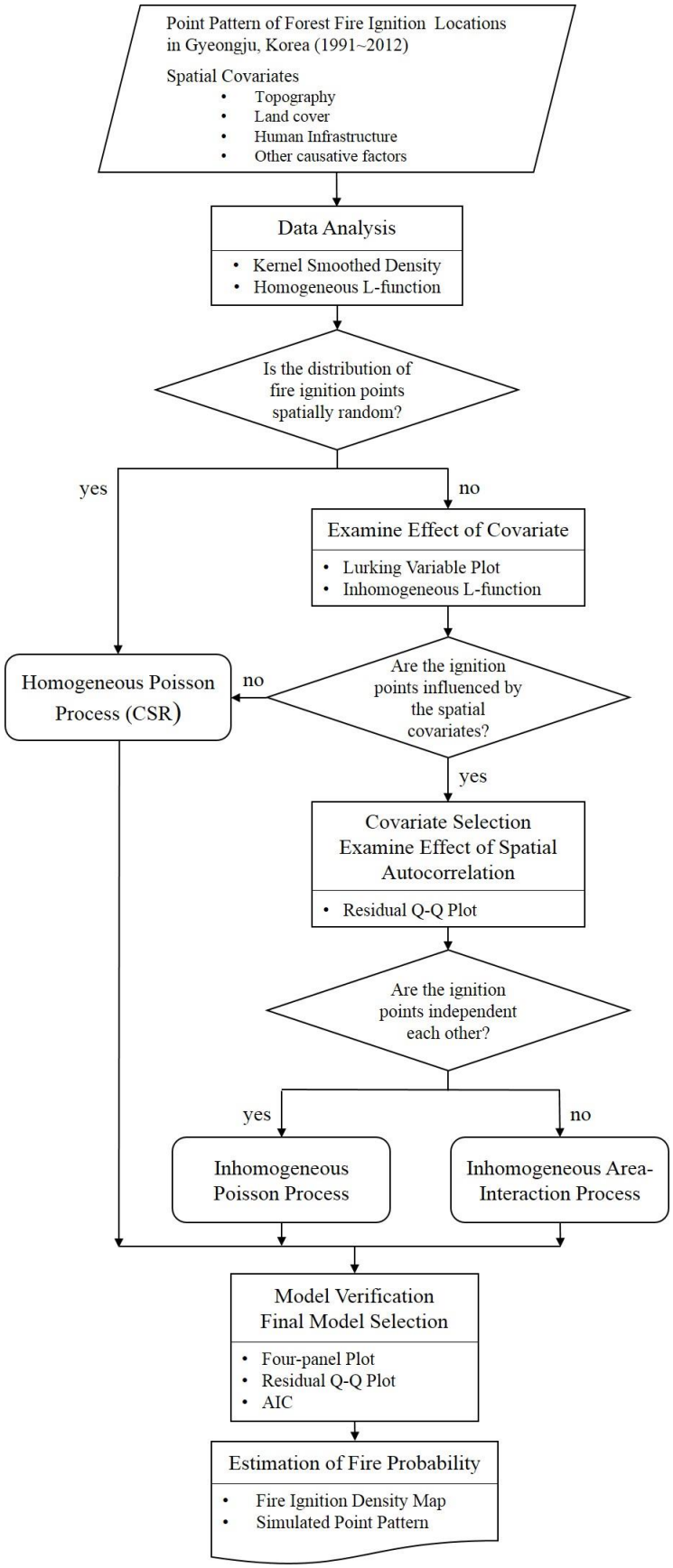
Point Pattern of Forest Fire Ignition Locations in Gyeongju, Korea (1991~2012)
Spatial Covariates
• Topography
• Land cover
• Human Infrastructure
• Other causative factors
Data Analysis
• Kernel Smoothed Density
• Homogeneous L-function
Is the distribution of fire ignition points spatially random?
yes
no
Examine Effect of Covariate
• Lurking Variable Plot
• Inhomogeneous L-function
Are the ignition points influenced by the spatial covariates?
no
Homogeneous Poisson Process (CSR)
yes
Covariate Selection
Examine Effect of Spatial Autocorrelation
• Residual Q-Q Plot
Are the ignition points independent each other?
yes
no
Inhomogeneous Poisson Process
Inhomogeneous Area-Interaction Process
Model Verification
Final Model Selection
• Four-panel Plot
• Residual Q-Q Plot
• AIC
Estimation of Fire Probability
• Fire Ignition Density Map
• Simulated Point Pattern

Figure 1.2. Flowchart for analyzing and modelling procedures of the point pattern of forest fire ignition locations in Gyoengju, Korea (1991~2012).

1.4 Study Landscape and Data Description

The study landscape, Gyeongju, is located in Gyeongsangbuk-do, in the southeast part of Korea (Figure 3). The geographic location of the study landscape ranges approximately from 128.58° E to 129.29° E, and from 35.38° N to 36.30° N. The entire landscape is about 1,320 km^2, including several urban areas with a total population of approximately 270,000 (Gyeongju-si, 2012). Almost 70% of the study landscape (i.e. 919.90 km^2) consists of forested lands. The landscape has a temperate climate, with primarily mixed forests and pine trees (*Pinus densiflora*) as the dominant tree species (Table 1). The elevation ranges widely, from sea level to 1,013 m (e.g. Mt. Moonbok, the west side of the region). The Hyeongsan-gang is a large river flowing longitudinally across the landscape.

There were a total of 142 forest fires reported in Gyeongju between 1991 and 2012, a period of 21 years (Figure 4a). The map coordinates of forest fire ignition points (including source of ignition) were obtained from the Korea Forest Service (KFS) and the Korea Forest Research Institute (KFRI).

The overall characteristics and trend of forest fires in the study landscape are summarized in Table 2 and Figure 5. The number of fires per year fluctuates, ranging from 1 to 16, although, recent fire prevention efforts, such as new restrictions on fire use during forest recreation activities and education programs, seem effective in reducing anthropogenic fire occurrences (Korea Forest Service, 2012). The majority of historical fires occurred in spring (March to May), the driest season in Korea. The leading cause of fires are hikers, accounting for over 57% of all occurrences. Incineration of waste or cropland residues ranks as the next highest cause at 20%.

Other spatial datasets for the landscape such as topography, forest stand type, community infrastructures, and local environment variables were also obtained from KFRI in the form of digitized maps. The digital elevation model (DEM), slope, and aspect of the study landscape were reclassified into raster data with a 100×100 m spatial resolution (Figure 4b, 4c, and 4d, respectively). The original forest stand type map included 17 classes of forest land cover based on dominant tree species. To simplify the data, we reclassified them into four major stand types: coniferous forests, deciduous forests, mixed forests, and non-forested areas (Table 1). The reclassified land cover was then rasterized into a 100 m-resolution raster dataset (Figure 4e). The aspect raster was also classified into three categorical variables: flat, low potential solar radiation (North, Northeast, Northwest, and East facing plane), and high potential solar radiation (Southeast, Southwest, South, and West facing plane). All geoprocessing operations were performed using ArcGIS 10.2 (ESRI, 2012).

To address the effects of human activity on forest fire occurrence, distances from roads and buildings were considered as explanatory variables. The maps of roads and buildings in the study landscape were obtained and rasterized into 100-m resolution grid cells with an attributed Euclidean distance from these map features (Figure 4f and 4g). The densities of tombs and croplands across the landscape were calculated per hectare and rasterized with the same resolution (Figure 4h and 4i). Since the distributions of these grid cell values (i.e. Euclidean distance to roads and buildings, densities of tombs and croplands) are heavily right-skewed, logarithmic transformations were performed for these values.

Table 1.1. Land classification in Gyeongju based on dominant tree species.

Dominant Species	Class	Percentage (%) of Total Forested Area
Pinus densiflora	Coniferous Forest	30.51
Pinus koraiensis		3.02
Pinus rigida		2.91
Larix kaempferi		2.81
Other coniferous species		0.09
Quercus	Deciduous Forest	0.08
Bambuseae		0.01
Camellia sinensis		0.01
Castanea crenata		<0.01
Other deciduous species		22.05
Mixed Forest	Mixed Forest	35.16
Grassland	Non-forested Area	0.97
Cultivated land		1.68
Wilderness		0.07
Others		0.63

Table 1.2. Distribution of forest fires by cause.

Cause	Number of Fire	Percentage (%)
Hikers	81	57.04
Incineration of Garbage & Croplands Residue	28	19.72
Tomb Visitors	10	7.04
Cigarettes	6	4.23
Arson	3	2.11
Others	14	9.86
Total	142	

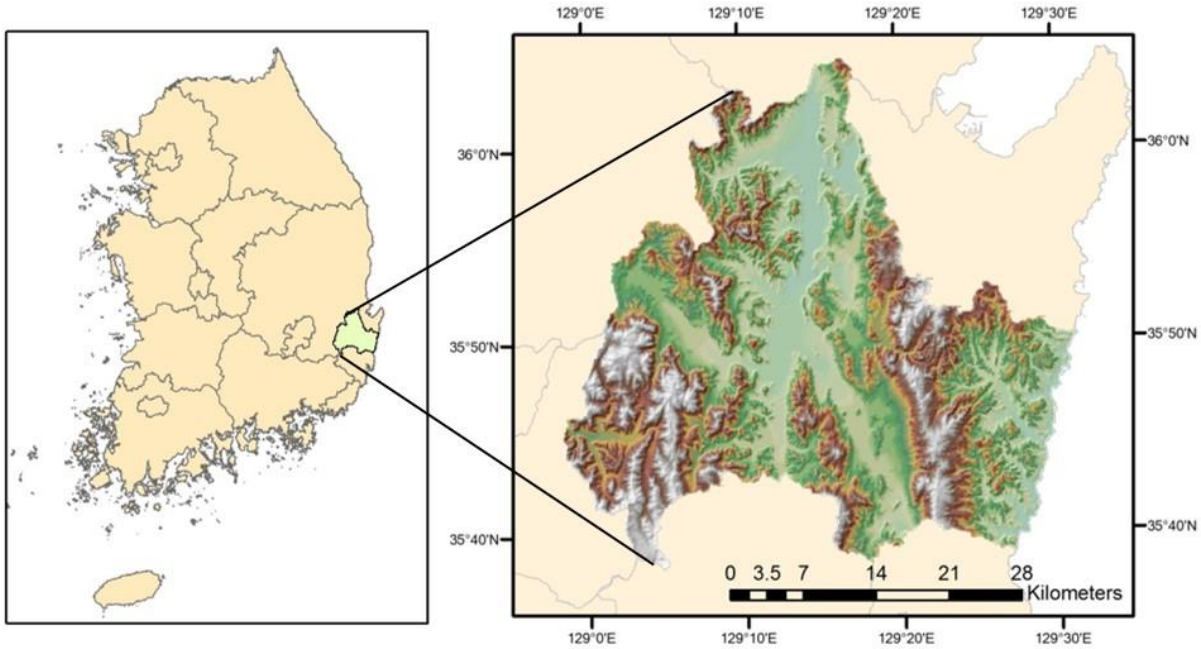

Figure 1.3. Study landscape of Gyeongju, located in Gyeongsangbuk-do, South Korea.

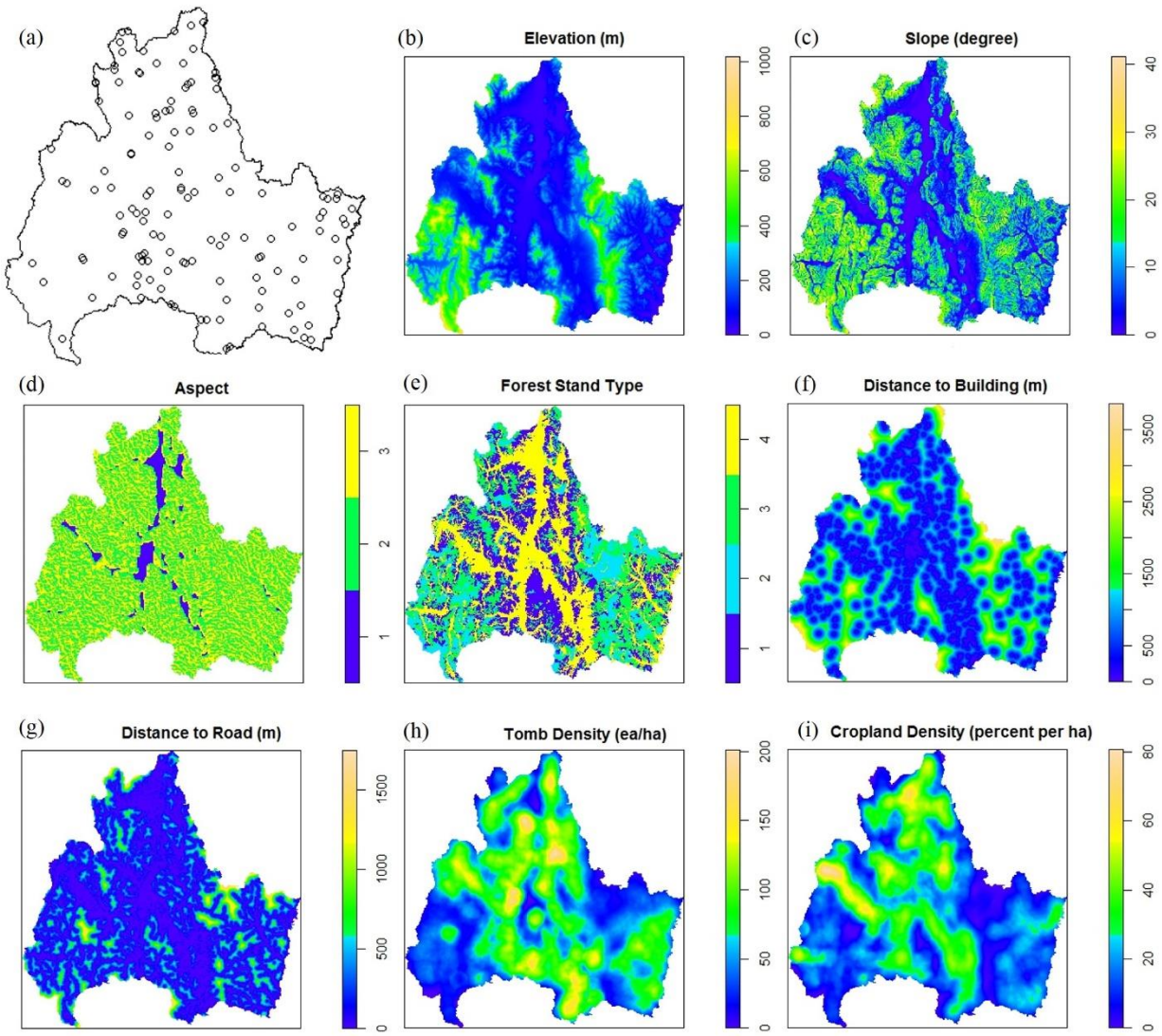

Figure 1.4. (a) Point pattern of forest fire ignition locations from 1991 to 2012 in Gyeongju, and (b through i) spatial distribution and range of eight covariates.

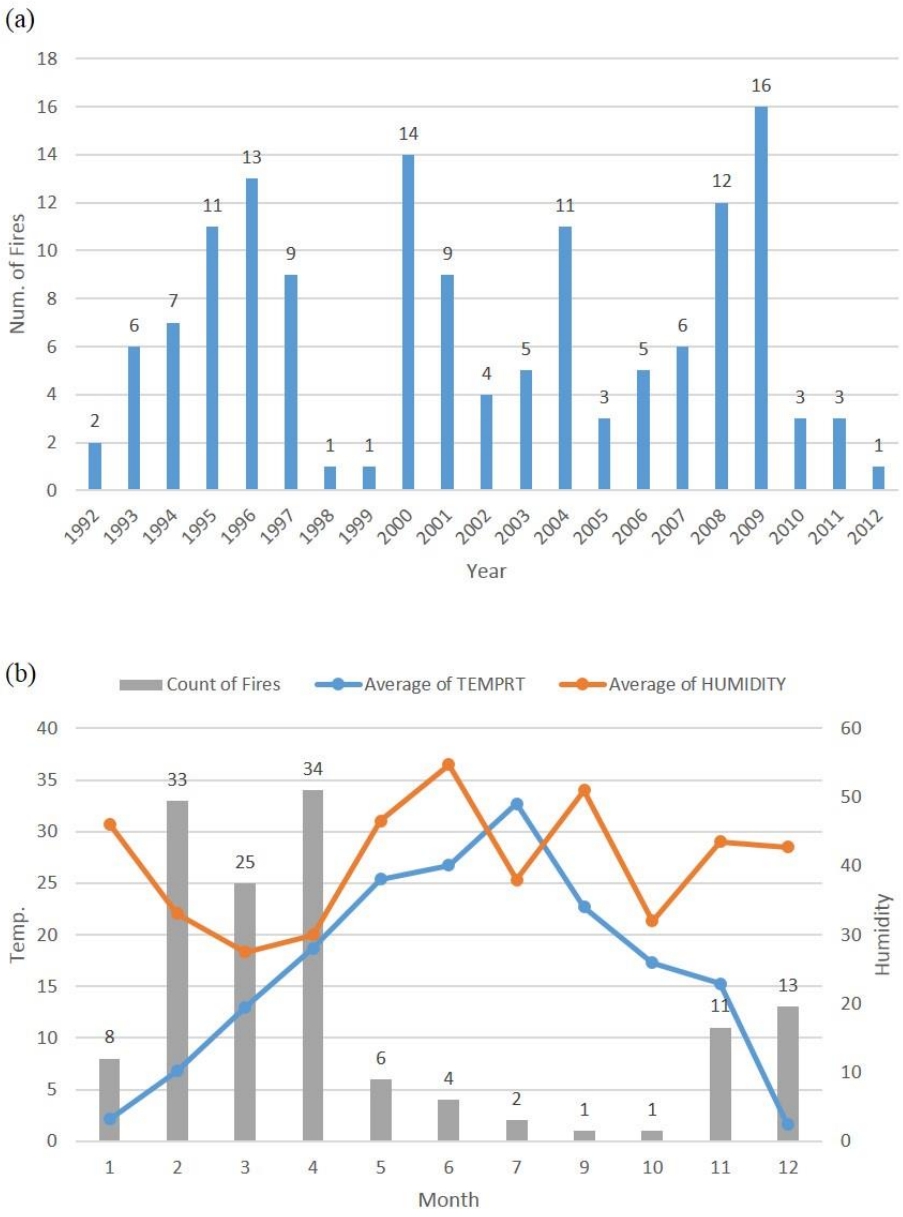

Figure 1.5. Annual and monthly distributions of forest fires in Gyeongju (a and b, respectively). The monthly distribution is presented with average temperature and humidity.

1.5 Results and Discussions

1.5.1 Homogeneous Poisson model

Assuming a null hypothesis of CSR, the accumulated intensity of forest fire ignition points across the landscape over 21 years (1991 to 2012) was 5.12×10^{-5} fires ha^{-1} year^{-1} on average. This means that every hectare cell in the landscape had approximately 0.005% probability of fire occurrence each year. The kernel smoothed density map of the forest fire ignition points (Figure 6) showed higher density at the upper and lower center of the study area. The far east of the study region experienced comparatively more frequent fire incidences, while the westernmost area exhibited the least amount of fires.

The comparison of the L-function (Figure 7a) between the observed point pattern and the null model (homogeneous Poisson process) indicates that the ignition points tend to be clustered (i.e. $L(r) > 0$). Notably, the departure from CSR escaping the pointwise confidence envelope appears at two different scales, e.g., at relatively close scale (range of 800~1400 meters from each ignition) and broad scale (over 3500 meters). This suggests that the complex clustering pattern may originate from different sources of aggregation, either from the effect of spatial trends or positive interactions between the ignition points.

Residuals of the null model are described by the four-panel plot in Figure 7b. The marked plot (upper left panel) displays the constant intensity ($\hat{\lambda}(\boldsymbol{u}) = 1.0143 \times 10^{-7}$) over the region. The smoothed residual field (lower right) and the lurking variable plots along with the x- and y-coordinates (lower left and upper right panels respectively) show large Pearson residuals (outside the 2-standard deviation limits, noted by the dotted line) in the western and mid-upper area of the study landscape. The intensity of fire ignition points on the west side is overestimated, which indicates poor fit of the homogeneous Poisson model.

These results indicate that the forest fire ignition points in Gyeongju are not randomly distributed. Rather, they are clustered over the region, and the homogeneous Poisson process is inadequate to explain the pattern of fire ignition. The spatially clustering pattern of forest fire ignition points may be induced either by spatial aggregation of fire-causative factors (i.e. trend), positive dependence among fire ignitions (i.e. interaction), or both.

1.5.2 Spatial Covariate Effects

Successful inclusion of spatial trends is determined by checking the dependence of ignition locations on individual covariates. Partial residual plots for candidate variables are commonly used to determine which variables should be included in a linear model. In a point process, the lurking variable plot which depicts the cumulative residuals against each covariate functions similarly (Baddeley et al., 2004). The residual function should be approximately zero if the fitted model is correct. If the cumulative residuals under CSR deviate far from zero (e.g. over 2σ of the residuals) for a particular covariate, the density of the point pattern is highly associated with the covariate and the covariate should be considered in the model as a predictor. The result of lurking variable plots (Figure 8) with six continuous spatial covariates (elevation, slope, distance to road, distance to building, tomb density, and croplands density) illustrates that fire ignition point density is dependent only on elevation, slope, distance to road, and tomb density. To be precise, the cumulative Pearson residuals for elevation under the hypothesis of CSR (Figure 8a) increase sharply from 70m to 250m, indicating that ignitions occur more frequently at this range, and are clustered at 200~400m of elevation. The density of ignition points is less than expected on lower slopes, only starting to increase at a slope of 8 degrees (Figure 8b), indicating that fires are less likely to ignite on flat topography. For the covariate of distance to road, the cumulative residual curves are below the -2σ threshold of error bounds (dotted line, $< 150\text{m}$ (i.e. $\log 5$) from the

road in Figure 8c), which implies that fewer forest fires occur within close proximity to a road. The density of ignition points is overestimated at sites with 15~150 (i.e. $\log 2.7 \sim \log 5$) tombs per ha^{-1} (Figure 8e) and the cumulative residuals increases rapidly after that, indicating the forest fire ignition is associated only with a high density of tombs. The categorical variables (forest stand and aspect) are both associated with density of fire ignition point. Coniferous forest lands experience more frequent fire occurrences when compared to deciduous, mixed forest and non-forested areas. South-facing terrain exhibits a higher density of ignition points relative to other aspects. Distance to buildings and cropland density were not found to be significant factors influencing the density of fire ignition points (Figure 8d and 8f).

Low elevation terrain is highly accessible to humans, and our results correspond with preconceived beliefs, as well as with many previous studies (e.g. Vega-García et al., 1993; Cardille et al., 2001; Syphard et al., 2008; Catry et al., 2010). South-facing aspects in northern hemisphere are more exposed to heat from sunlight, and this condition is in favor of fire ignition. Increased susceptibility of coniferous forests to forest fire has already been well documented in previous research (e.g. Chou et al., 1993; Bar Massada et al., 2009). Given the primary causes of forest fires (Table 2), it seems reasonable that areas with higher tomb densities maintain a higher likelihood of fire ignition. However, it was unexpected to find that the covariates of distance to road and slope are positively associated with the density of forest fires. We speculate the reason for this is that the road coverage used in this study contains only major road networks, excluding forest roads or trails that are typically used by hikers. Because hiking trails likely do not coexist with major traffic roads, the Euclidean distance from trails to roads may be large. This may partly explain higher fire ignition in remote areas from the existing roads. Gentle slope areas are usually used for

residential or agricultural lands, and this seems to be reflected in the low forest fire ignition potential.

1.5.3 Inhomogeneous Poisson model

We proceeded to include the selected covariates (elevation, slope, aspect, forest stand, distance to road and tombs density) as potential predictors of spatial trend in an inhomogeneous Poisson model. The results of fitting this model are provided in Table 3 and Figure 9. The lurking variable plots plotted against each selected covariate (Figure 9) show that the effect of the covariates are successfully accounted for as part of the spatial trend, except for a slight overfitting of the slope variable (Figure 9b).

A 95% pointwise confidence band for the L-function obtained by 200 Monte Carlo simulations (grey area) captured the majority of observed L-statistics (black solid line, Figure 10a) when compared to those of the homogeneous Poisson model (Figure 7a). This suggests that the majority of the clusters from the ignition point pattern on our study landscape can be explained by the modeled spatial trend. It is worth noting that the extra clustering observed at broad scales (over 3500 meters in Figure 7a) is well-explained by the fitted model, while there remains some clustering at closer scales (1000~1200 meters in Figure 7a). The AIC value for the inhomogeneous Poisson model (AIC=4552.4) is considerably smaller than that for the null model (AIC=4585.8) (Table 4), exhibiting improvement as a model for ignition point density.

Four-panel residual analysis was also conducted (Figure 10b) to check goodness-of-fit of the inhomogeneous Poisson model. In comparison with the homogeneous Poisson model, the vertical and horizontal sums of Pearson residuals (lower left and upper right panels in Figure 10b) show reduced model lack of fit after incorporating the spatial covariates. However, some deviations of residuals from the inhomogeneous model at the upper-center part of the region still

exist, located around [390000, 280000] metric coordinate (lower right panel in Figure 10b). This suggests either the possibility of misspecification of current spatial covariates or the need for additional covariates associated with the density of fire ignition points, or interaction among the points.

The Q-Q plot for the residual distribution (Figure 11a) assists in detecting possible interpoint interaction by comparing empirical quantiles of the smoothed residual field and expected quantiles under the fitted model. The circles represent empirical quantiles of the smoothed residual field for the original data against expected quantiles of the corresponding order statistic under the inhomogeneous Poisson model. The expected quantiles are supplied by calculating the sample mean of ordered residuals obtained by multiple simulated realizations of the fitted model, i.e., 100 iterations of Monte Carlo simulation. The distribution of empirical residual data shows marginal fit to the 95% prediction intervals of the inhomogeneous Poisson model (the red dotted lines) with a slightly longer right tail and more variability. This indicates a positive interaction between the points.

Combined, these findings indicate that clustering of fire ignition point patterns only at close scales (1000~1200 meters in Figure 7a) may be accounted for by an attractive interpoint interaction. Therefore, we introduced the effect of this interaction (i.e. spatial autocorrelation) into the fire ignition density model.

1.5.4 Inhomogeneous area-interaction model

In order to fit a non-Poisson model containing interaction terms, the range of interaction (i.e. radius r from each point) needs to be determined. Generally the decision is made rather intuitively and heuristically, since no theoretical estimation or particular optimization method has been established (Mølle and Waagepetersen, 2007). We tested several disk radii r (e.g. $r =$

$100, 200, 500, 1000,$ and $2000\ m$), and selected $r = 500m$ because it produced the best result based on diagnostic plots.

The results of fitting an inhomogeneous area-interaction model to the given point pattern with the specified interaction radius $r = 500m$ are summarized in Table 3. The calculated interaction parameter γ is larger than 1 (Table 3, $\gamma = 2.3553$ with $p < 0.0001$ in a likelihood ratio test) as expected. This indicates strong evidence of additional attraction between fire ignition points within a radius of 500m from each ignition point given the spatial covariates. The pointwise confidence envelopes for the inhomogeneous L-function for the modeled area-interaction process successfully capture the observed L-statistics (Figure 12a) even at short ranges (1000~1200m) where the inhomogeneous Poisson model failed to provide an adequate model (refer to Figure 10a). The radius for broad scale clustering of ignition points (3500 meters and greater) is accounted for by the inhomogeneous Poisson process, while close scale clustering around 1000 m range is removed after the incorporation of this neighborhood effect. In an area-interaction process this can be interpreted as broad-scale clustering representing the effects of spatial trend, while relatively close-scale clustering results from positive dependence between ignition points.

The recognition of forest fire ignition locations as clustered point patterns agrees with previous studies (e.g. Podur et al., 2003; Yang et al., 2007; Turner, 2009; Juan et al., 2012). However, there has been little effort to differentiate the small-scale interactive behavior from large-scale trend-based aggregation. It is difficult to distinguish spatial autocorrelation and spatial trend (Legendre, 1993), and therefore aggregation in point patterns is often regarded as a result of environmental heterogeneity through a univariate analysis (Perry et al., 2006). Our results suggest a potential distinction between spatial trend and autocorrelation by means of modeling the inhomogeneity at different scales.

Figure 12b illustrates the four-panel residual analysis of the area-interaction model. The statistical package used throughout this study does not support significance bands for lurking variable residual plots for non-Poisson models. Hence, a direct reading from the plot is unavailable. Nevertheless, relative comparisons with Figure 10b indicate that the goodness-of-fit of the inhomogeneous area-interaction model is even better than for the inhomogeneous Poisson model, demonstrated by the mitigation of point intensity overestimates near the top center of the region. The Q-Q plot for the smoothed residuals of the area-interaction model (Figure 11b) displays an adequate fit relative to by the 95% confidence bands, indicating that the incorporation of the interaction term is appropriate to offset additional clustering detected in the inhomogeneous Poisson model.

A slight deviation of Pearson residuals from zero still exists around the center top of the region (e.g., [405000, 290000] metric coordinates of lower right panel in Figure 12b), suggesting that there is still unexplained variation in the density of ignition points. This may be due to unknown variables which are not included in our model, such as population density and microclimate condition. However, since it is infeasible to assess the effects of every possible covariate and the unexplained variation is greatly reduced by the construction of the model, we assert that the area-interaction model allows more reliable predictions of fire occurrence probability.

The AIC value of the area-interaction model is 4230.025, which is considerably smaller than that of the inhomogeneous Poisson model (4552.422) (Table 4). It should be noted, however, that the maximized log-pseudolikelihood approximation is used here to calculate the AIC value as it is difficult to compute the log-likelihood for non-Poisson models (Huang and Ogata, 2002). This

implies that a direct comparison between the Poisson and non-Poisson model based on the AIC value might be misleading.

1.5.5 Model selection

Comparisons among the different point process models for the fire ignition point density in Gyeongju are summarized in Table 4 based on their log-likelihood and AIC values. The spatial logistic regression model slightly outperforms the inhomogeneous Poisson point process model when the same covariates are included. If the interaction term is added, however, the point process model can be more efficient than the logit model, especially when the spatial weight matrices are hard to derive directly. Again, the log-pseudolikelihood for the area-interaction model may be incomparable to the log-likelihood in the Poisson process or logistic regression model. In general, the use of log-likelihood estimators are recommended over the log-pseudolikelihood for stability and unbiasedness, although the log-pseudolikelihood estimators can also be unbiased and consistent under certain conditions. Unfortunately, the application of a log-likelihood for the non-Poisson point process model is not yet viable (Baddeley and Turner, 2000).

Considering the overall model performance and fitness discussed earlier, it is clear that the area-interaction point process model with a trend to account for the inhomogeneity performs the best of the three models. The predicted fire ignition point density of the study landscape and a realization of the fire ignition point pattern under the final model are provided in Figure 13. These estimation and simulation results are expected to be integrated into forest fire management planning as well as further research, such as the analysis of fire propagation to assess fire risks across a landscape.

Table 1.3. Summary of spatial covariates and interaction fitted in inhomogeneous Poisson model, inhomogeneous area-interaction model, and spatial logistic regression model.

		Inhomogeneous Poisson		**Inhomogeneous Area-interaction (r=500m)**		**Spatial Logistic Regression**	
Variables		**Fitted Coefficient**	**S.E.**	**Fitted Coefficient**	**S.E.**	**Fitted Coefficient**	**S.E.**
Intercept		-18.0945	1.3390	-18.5274	1.6830	-16.8252	1.2947
Forest Stand	Coniferous	N/A	N/A	N/A	N/A	N/A	N/A
	Deciduous	-0.6280	0.3493	-0.4303	0.3607	-0.7064	0.3535
	Mixed	-0.3611	0.2266	-0.3671	0.2843	-0.3098	0.2164
	Non-forested area	-0.8028**	0.2654	-0.7163**	0.2802	-1.2980**	0.2803
Aspect	Flat	N/A	N/A	N/A	N/A	N/A	N/A
	South-face	1.6601	1.0313	1.5697	1.0492	1.4889	1.0131
	North-face	1.4143	1.0318	1.3242	1.0508	1.3260	1.0123
Elevation		-0.0028**	0.0011	-0.0024**	0.0010	-0.0037**	0.0011
Slope		0.0152`	0.0159	0.0079	0.0172	0.0103	0.0160
Distance to Roads		0.0810*	0.0394	0.0811*	0.0468	0.0503*	0.0374
Tombs Density		0.2294`	0.1973	0.2922`	0.2423	0.0591	0.1871
Interaction		-	-	2.3733***	0.7670	-	-

*** p<0.001 ** p<0.01 * p<0.1 `

Table 1.4. Comparison of AIC and log-likelihood values among the models. Note that log-pseudolikelihood is presented for area-interaction model.

Model	**Structure**	**D.F.**	**AIC**	**Log-likelihood**
Homogeneous Poisson	-	1	4585.849	-2291.925
Inhomogeneous Poisson	Trend	10	4552.422	-2266.211
Logistic regression	Trend	10	4524.901	-2252.451
Area-interaction (r=500m)	Trend + Interaction	11	4230.025	-2104.012

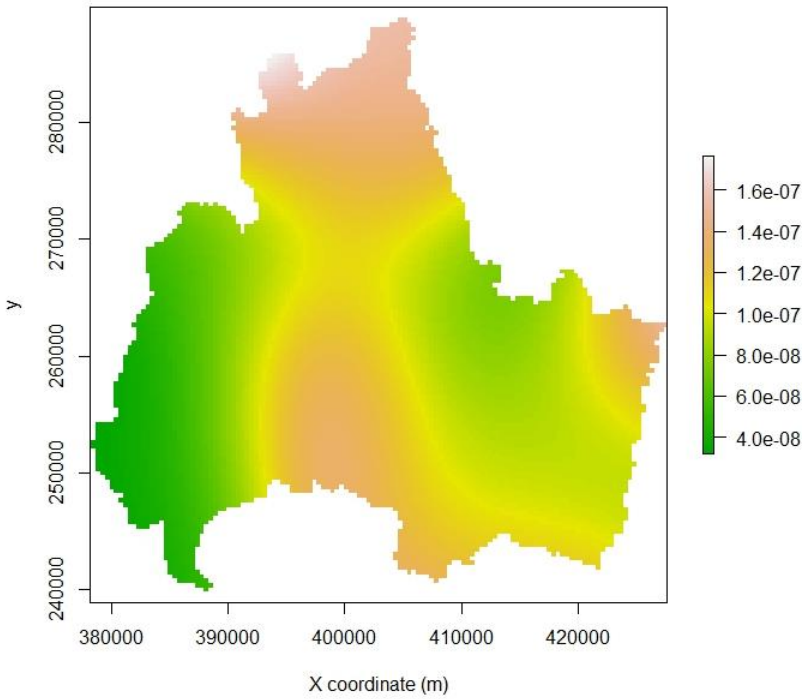

Figure 1.6. Kernel smoothed density (points per m^2) for the forest fire ignition data in Gyeongju, from 1991 to 2012.

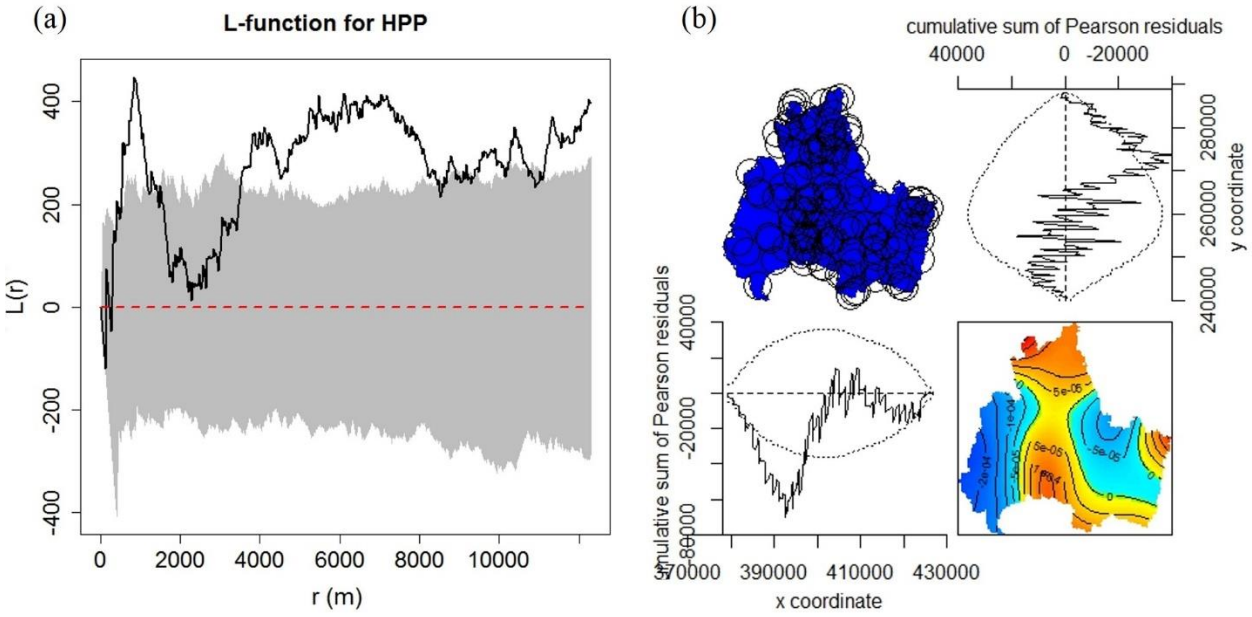

Figure 1.7. L-function for the fire ignition point pattern in Gyeongju observed from 1991 to 2012 (solid line in Figure 7(a)) and estimated 95% pointwise confidence envelope (grey area) for the homogeneous Poisson process (red dashed line in Figure 7(a)). The envelope was obtained through 200 Monte Carlo simulations. Four-panel Pearson residual plot for the homogeneous Poisson process (b).

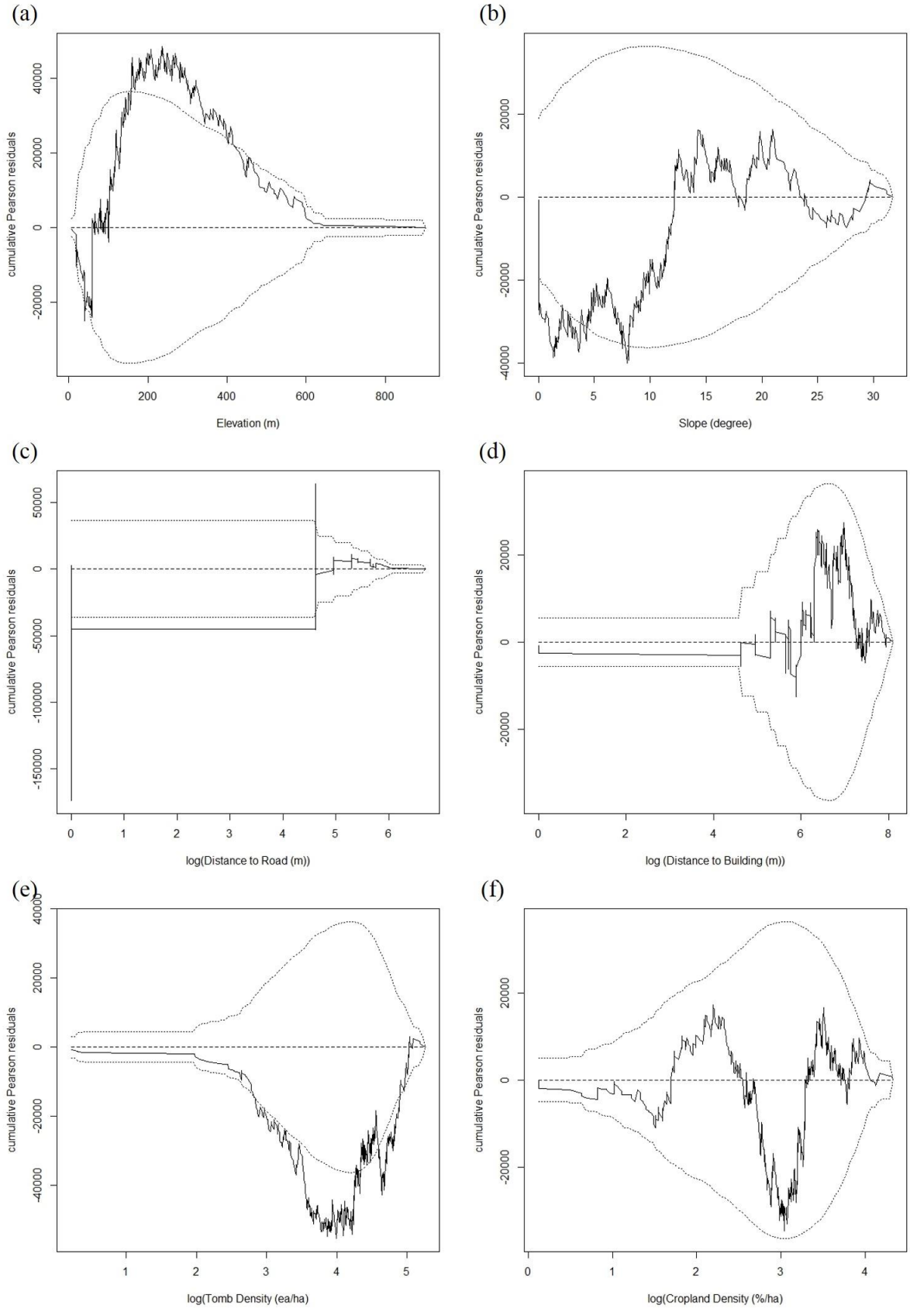
(a)
cumulative Pearson residuals
40000
20000
0
-20000
0
200
400
600
800
Elevation (m)
(b)
cumulative Pearson residuals
20000
0
-20000
-40000
0
5
10
15
20
25
30
Slope (degree)
(c)
cumulative Pearson residuals
50000
0
-50000
-100000
-150000
0
1
2
3
4
5
6
log(Distance to Road (m))
(d)
cumulative Pearson residuals
20000
0
-20000
0
2
4
6
8
log (Distance to Building (m))
(e)
cumulative Pearson residuals
40000
20000
0
-20000
-40000
1
2
3
4
5
log(Tomb Density (ea/ha)
(f)
cumulative Pearson residuals
20000
0
-20000
0
1
2
3
4
log(Cropland Density (%/ha)

Figure 1.8. Lurking variable plots depicting cumulative Pearson residuals against the following six spatial covariates: above sea level elevation in meters (a), slope in degrees (b), distance to road in meters (c), distance to buildings in meters (d), tombs density per hectare (e), and croplands density in % per ha (f). Note that the variables of distance to road, distance to buildings, tombs density and croplands density are in a log scale. The solid line represents observed residual values, and the dashed lines are 2σ error bounds for CSR.

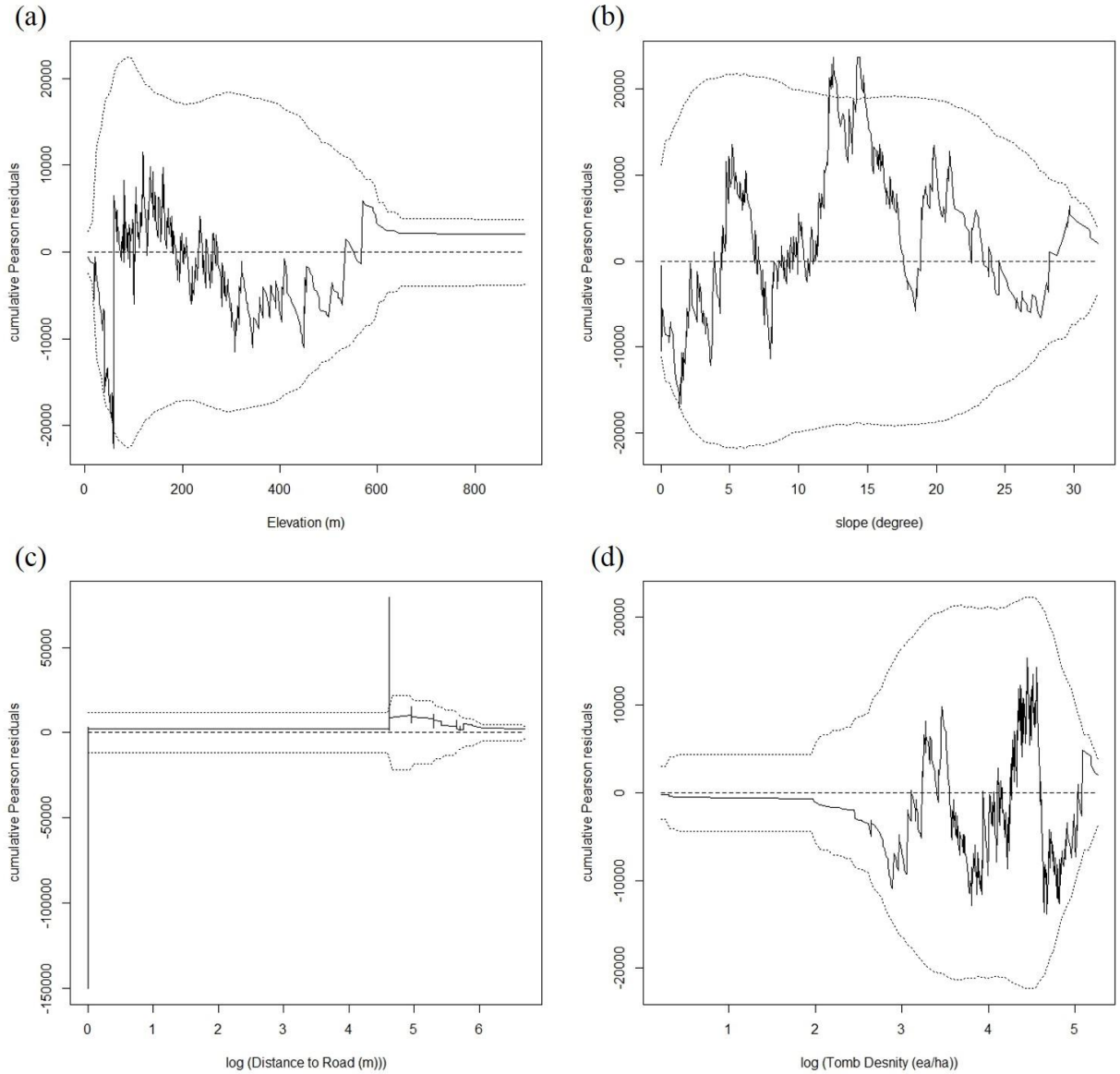

Figure 1.9. Lurking variable plots of cumulative Pearson residuals against selected spatial covariates under fitted inhomogeneous Poisson model including above sea level elevation in meters (a), slope in degrees (b), distance to road in meters (c), and tombs density per hectare (d). Note that the variables of distance to road and tombs density per hectare are in a log scale. The solid line represents observed residual values, and the dashed lines are 2σ error bounds for IPP.

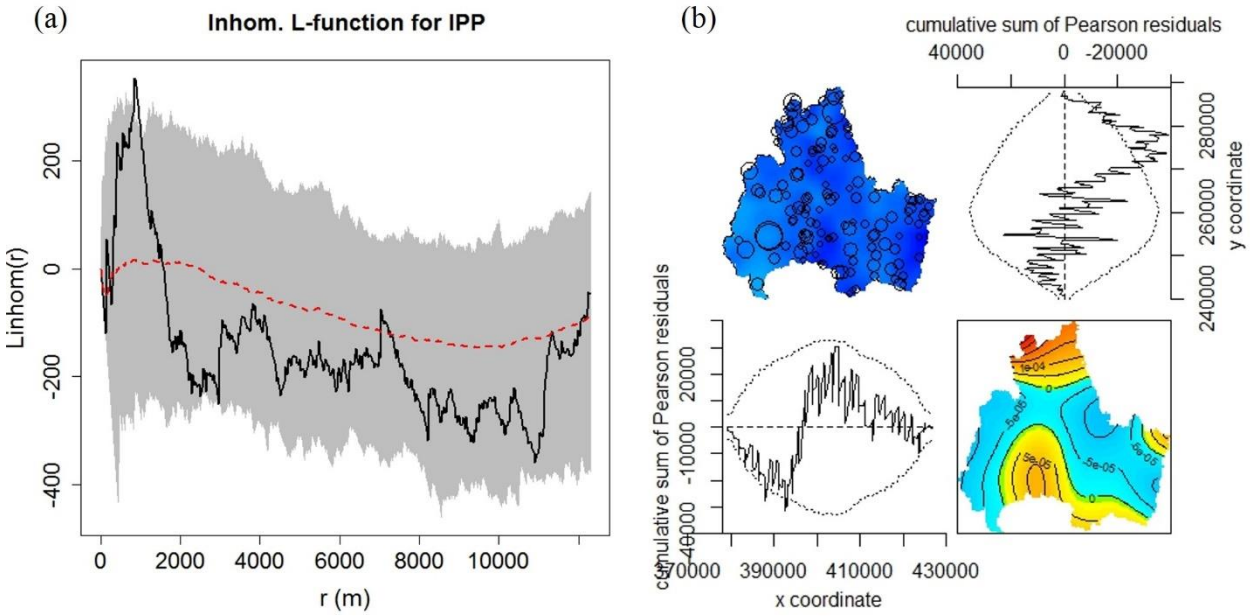

Figure 1.10. Inhomogeneous L-function for the empirical fire ignition point pattern (solid line in Figure 10a) and estimated 95% pointwise confidence envelope (grey area in Figure 10a) for the inhomogeneous Poisson process with six spatial covariates (red dashed line in Figure 10a). The envelope was obtained through 200 Monte Carlo simulations. Four-panel Pearson residual plot for the inhomogeneous Poisson model (b).

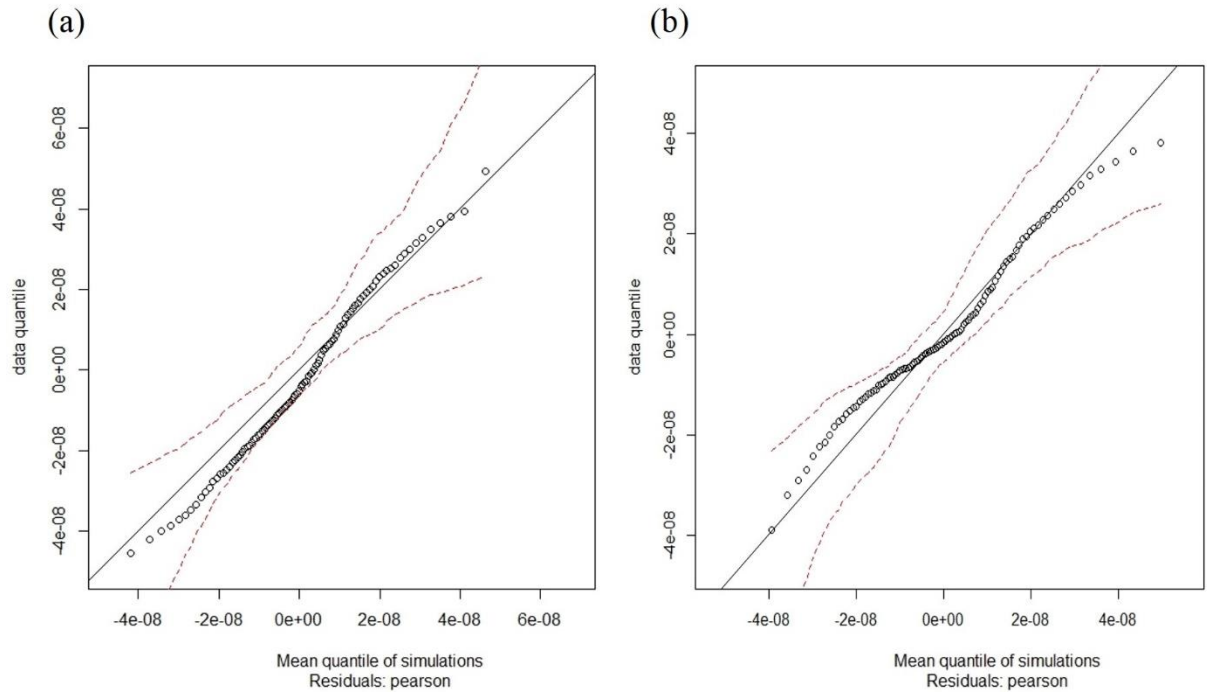

Figure 1.11. Residual Q-Q plots for the inhomogeneous Poisson model (a), and inhomogeneous area-interaction model when $r = 500m$ (b). The smoothed residual fields are dotted against the average of expected empirical quantiles obtained by 100 simulations under each fitted model. Dashed lines represent 95% prediction intervals.

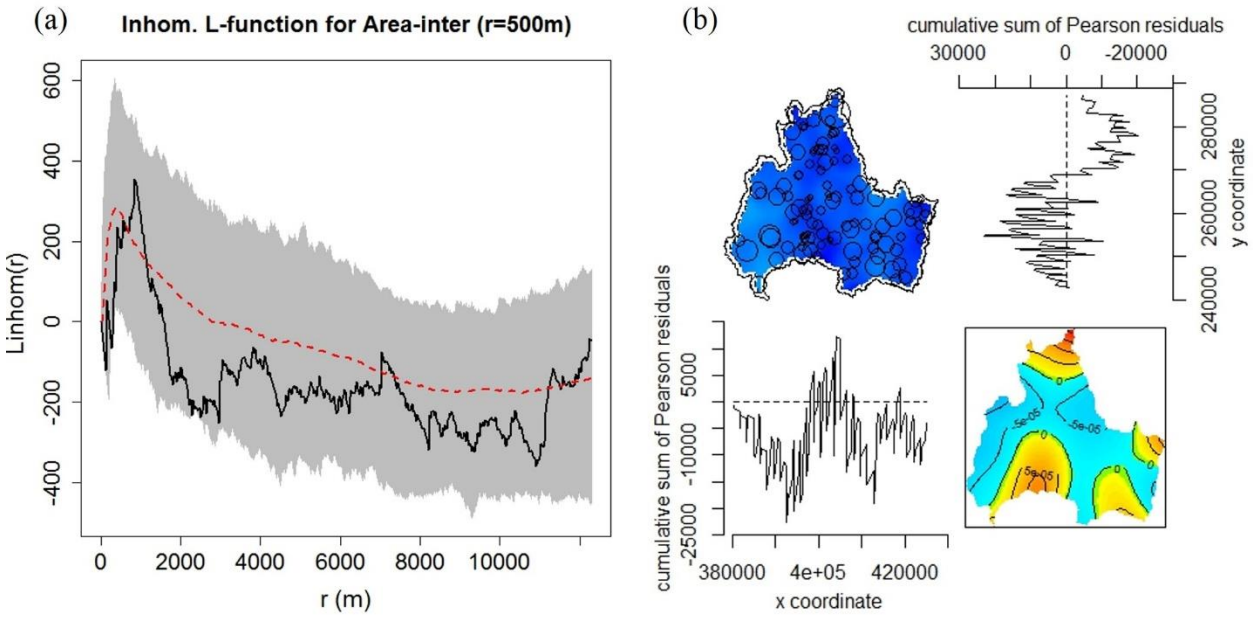

Figure 1.12. Inhomogeneous L-function for the empirical fire ignition point pattern (solid line in Figure 12 a) and estimated 95% pointwise confidence envelope (grey area in Figure 12a) for the inhomogeneous area-interaction process with the range of neighborhood $r = 500m$ and six spatial covariates (red dashed line in Figure 12a). The envelope was obtained through 200 Monte Carlo simulations. Four-panel Pearson residual plot for the inhomogeneous area-interaction process (b).

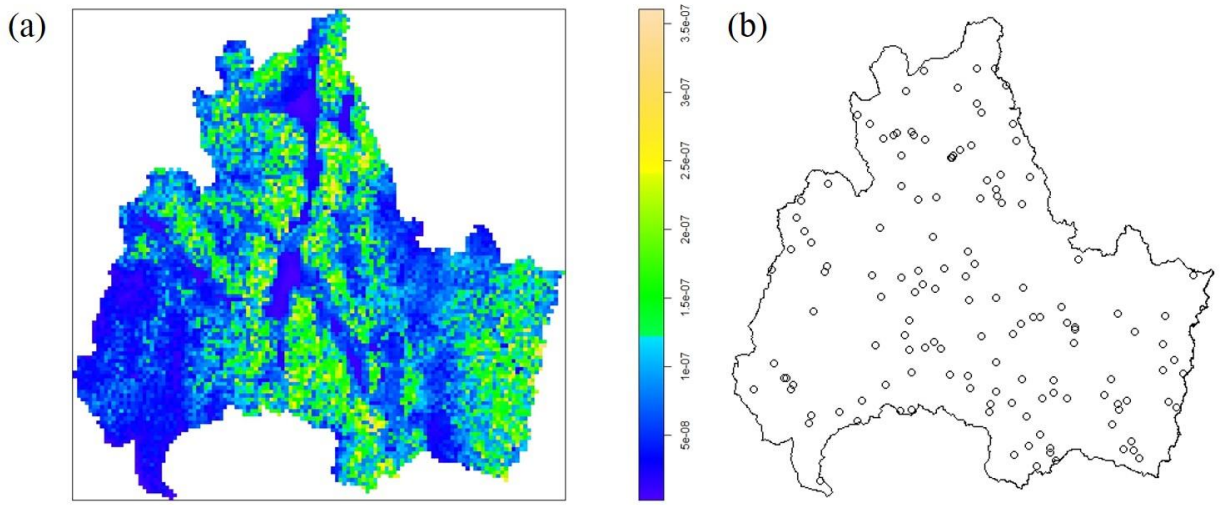

Figure 1.13. Predicted forest fire ignition point density based on the final model (i.e. inhomogeneous area-interaction process with $r = 500m$) (a), one realization of point pattern provided by implementation of the final model (b).

1.6 Conclusion

In this study, we modeled the density of forest fire ignition points in Gyeongju, Korea using SPP models. The modeling process was designed to derive fire occurrence probability in terms of spatial covariates such as topography and land cover of the study landscape, and in terms of spatial dependence between the ignition points themselves. The distribution of fire ignition points was clustered depending on spatial inhomogeneity of the covariates involved, and exhibited positive spatial autocorrelation among the locations of ignition points. The results indicate that the inhomogeneous area-interaction model, which contains both spatial covariates and local neighborhood effects is the most informative when compared to the other models tested. A map of forest fire ignition point density predicted by the final model and a possible set of estimated ignition locations were developed as the result of this study.

The utilization of SPP models allows direct incorporation of spatial trends and autocorrelations within a model, yielding flexible models such as the inhomogeneous Poisson model and the Markov point process area-interaction model. In comparison with the spatial logistic regression model, the area-interaction model seemed to perform better. Although the comparison does not provide numerical evidence, use of a SPP appears to be the best choice when addressing "presence-only data" (such as fire occurrence data), owing to its more sensible model specification, and ease of interpretation and implementation (Warton and Shepherd, 2010). The potential of point process models will be fully identified in the future as new methodological developments are underway.

Spatial prediction of forest fire ignition probability can provide useful information not only for fire management planning and resource allocation for fire suppression activities, but also as a stepping stone for further research. The second portion of this research utilizes the density of fire

ignition to produce a plausible set of ignition points for multiple fire simulations and estimate the burn probability of each pixel across the landscape. The details of the second part of this study are described in the next chapter.

1.7 References

Akaike, H. (1974). A new look at the statistical model identification. *Automatic Control, IEEE Transactions on*, 19(6), 716-723.

Baddeley, A. J., Møller, J., & Waagepetersen, R. (2000). Non-and semi-parametric estimation of interaction in inhomogeneous point patterns. *Statistica Neerlandica*, 54(3), 329-350.

Baddeley, A. J., & Turner, R. (2004). Spatstat: An R Package for Analyzing Spatial Point Pattens.

Baddeley, A. J., & Van Lieshout, M. N. M. (1995). Area-interaction point processes. *Annals of the Institute of Statistical Mathematics*, 47(4), 601-619.

Baddeley, A., & Turner, R. (2000). Practical maximum pseudolikelihood for spatial point patterns. *Australian & New Zealand Journal of Statistics*, 42(3), 283-322.

Baddeley, A., Turner, R., Møller, J., & Hazelton, M. (2004). Residual analysis for spatial point processes. *AMS Clasification*.

Bar Massada, A., Radeloff, V. C., Stewart, S. I., & Hawbaker, T. J. (2009). Wildfire risk in the wildland–urban interface: a simulation study in northwestern Wisconsin. *Forest Ecology and Management*, 258(9), 1990-1999.

Berman, M., & Turner, T. R. (1992). Approximating point process likelihoods with GLIM. *Applied Statistics*, 31-38.

Besag, J. E. (1977). Comments on Ripley's paper. *Journal of the Royal Statistical Society B*, 39(2), 193-195.

Besag, J., Milne, R., & Zachary, S. (1982). Point process limits of lattice processes. *Journal of Applied Probability*, 210-216.

Bozdogan, H. (1987). Model selection and Akaike's information criterion (AIC): The general theory and its analytical extensions. *Psychometrika*, 52(3), 345-370.

Bradley, A. F., Noste, N. V., & Fischer, W. C. (1992). Fire ecology of forests and woodlands in Utah.

Cardille, J. A., Ventura, S. J., & Turner, M. G. (2001). Environmental and social factors influencing wildfires in the Upper Midwest, United States. *Ecological Applications*, 11(1), 111-127.

Catry, F. X., Rego, F. C., Bação, F. L., & Moreira, F. (2010). Modeling and mapping wildfire ignition risk in Portugal. *International Journal of Wildland Fire*, 18(8), 921-931.

Chou, Y. H., Minnich, R. A., & Chase, R. A. (1993). Mapping probability of fire occurrence in San Jacinto Mountains, California, USA. *Environmental Management*, 17(1), 129-140.

Cox, D. R., & Isham, V. (1980). *Point processes* (Vol. 12). CRC Press.

Diggle, P. J. (1983). *Statistical analysis of spatial point patterns*. Academic Press.

ESRI 2012. ArcGIS Desktop: Release 10.2. Redlands, CA: Environmental Systems Research Institute.

Garcia, C. V., Woodard, P. M., Titus, S. J., Adamowicz, W. L., & Lee, B. S. (1995). A logit model for predicting the daily occurrence of human caused forest-fires. *International Journal of Wildland Fire*, 5(2), 101-111.

Genton, Marc G.; Butry, David T.; Gumpertz, Marcia L.; Prestemon, Jeffrey P. (2006). Spatio-temporal analysis of wildfire ignitions in the St. Johns River Water Management District, Florida. *International Journal of Wildland Fire*. 15: 87-97.

Hering, A. S., Bell, C. L., & Genton, M. G. (2009). Modeling spatio-temporal wildfire ignition point patterns. *Environmental and Ecological Statistics*, 16(2), 225-250.

Huang, F., & Ogata, Y. (2002). Generalized pseudo-likelihood estimates for Markov random fields on lattice. *Annals of the Institute of Statistical Mathematics*, 54(1), 1-18.

Illian, J., Penttinen, A., Stoyan, H., & Stoyan, D. (2008). *Statistical analysis and modelling of spatial point patterns* (Vol. 70). John Wiley & Sons.

Juan, P., Mateu, J., & Saez, M. (2012). Pinpointing spatio-temporal interactions in wildfire patterns. *Stochastic Environmental Research and Risk Assessment*, 26(8), 1131-1150.

Kelly, F. P., & Ripley, B. D. (1976). A note on Strauss's model for clustering. *Biometrika*, 357-360.

Korea Forest Service. (2012). *Statistical Yearbook of Forestry 2012*, Daejeon, Republic of Korea

Law, R., Illian, J., Burslem, D. F., Gratzer, G., Gunatilleke, C. V. S., & Gunatilleke, I. A. U. N. (2009). Ecological information from spatial patterns of plants: insights from point process theory. *Journal of Ecology*, 97(4), 616-628.

Lee, B., Park, P. S., & Chung, J. (2006). Temporal and spatial characteristics of forest fires in South Korea between 1970 and 2003. *International Journal of Wildland Fire*, 15(3), 389-396.

Legendre, P. (1993). Spatial autocorrelation: trouble or new paradigm?. *Ecology*, 74(6), 1659-1673.

Lloyd, O. L., Smith, G., Lloyd, M. M., Holland, Y., & Gailey, F. (1985). Raised mortality from lung cancer and high sex ratios of births associated with industrial pollution. *British journal of industrial medicine*, 42(7), 475-480.

Mercer, D. E., & Prestemon, J. P. (2005). Comparing production function models for wildfire risk analysis in the wildland–urban interface. *Forest Policy and Economics*, 7(5), 782-795.

Møller, J., & Waagepetersen, R. P. (2007). Modern statistics for spatial point processes*. *Scandinavian Journal of Statistics*, 34(4), 643-684.

Ogata, Y. (1998). Space-time point-process models for earthquake occurrences. *Annals of the Institute of Statistical Mathematics*, 50(2), 379-402.

Papangelou, F. (1974). The conditional intensity of general point processes and an application to line processes. *Probability Theory and Related Fields*, 28(3), 207-226.

Pearce, J. L., & Boyce, M. S. (2006). Modelling distribution and abundance with presence-only data. *Journal of Applied Ecology*, 43(3), 405-412.

Perry, G. L., Miller, B. P., & Enright, N. J. (2006). A comparison of methods for the statistical analysis of spatial point patterns in plant ecology. *Plant Ecology*, 187(1), 59-82.

Pew, K. L., & Larsen, C. P. S. (2001). GIS analysis of spatial and temporal patterns of human-caused wildfires in the temperate rain forest of Vancouver Island, Canada. *Forest ecology and management*, 140(1), 1-18

Picard, N., BAR-HEN, A. V. N. E. R., Mortier, F., & Chadoeuf, J. (2009). The multi-scale marked area-interaction point process: A model for the spatial pattern of trees. *Scandinavian journal of statistics*, 36(1), 23-41.

Podur, J., Martell, D. L., & Csillag, F. (2003). Spatial patterns of lightning-caused forest fires in Ontario, 1976–1998. *Ecological Modelling*, 164(1), 1-20.

Preisler, H. K., Brillinger, D. R., Burgan, R. E., & Benoit, J. W. (2004). Probability based models for estimation of wildfire risk. *International Journal of Wildland Fire*, 13(2), 133-142.

Prestemon, J. P., & Butry, D. T. (2005). Time to burn: modeling wildland arson as an auto-regressive crime function. *American journal of agricultural economics*, 87(3), 756-770.Prestemon, J. P., Hawbaker, T. J., Bowden, M., Carpenter, J., Brooks, M. T., Abt, K. L., ... & Scranton, S. (2013). Wildfire ignitions: A review of the science and recommendations for empirical modeling.

Ripley, B. D. (1977). Modelling spatial patterns. *Journal of the Royal Statistical Society B (Methodological)*, 172-212.

Ripley, B. D. (1991). *Statistical inference for spatial processes*. Cambridge university press.

Romero-Calcerrada, R., Novillo, C. J., Millington, J. D. A., & Gomez-Jimenez, I. (2008). GIS analysis of spatial patterns of human-caused wildfire ignition risk in the SW of Madrid (Central Spain). *Landscape Ecology*, 23(3), 341-354.

Stein, A., & Georgiadis, N. (2006). Spatial marked point patterns for herd dispersion in a savanna wildlife herbivore community in Kenya. In *Case studies in spatial point process modeling* (pp. 261-273). Springer New York.

Stoyan, D., & Penttinen, A. (2000). Recent applications of point process methods in forestry statistics. *Statistical Science*, 61-78.

Strauss, D. J. (1975). A model for clustering. *Biometrika*, 62(2), 467-475.

Syphard, A. D., Radeloff, V. C., Keuler, N. S., Taylor, R. S., Hawbaker, T. J., Stewart, S. I., & Clayton, M. K. (2008). Predicting spatial patterns of fire on a southern California landscape. *International Journal of Wildland Fire*, 17(5), 602-613.

Turner, R. (2009). Point patterns of forest fire locations. *Environmental and ecological statistics*, 16(2), 197-223.

Uria-Diez, J., Ibáñez, R., & Mateu, J. (2013). Importance of habitat heterogeneity and biotic processes in the spatial distribution of a riparian herb (*Carex remota L.*): a point process approach. *Stochastic Environmental Research and Risk Assessment*, 27(1), 59-76.

Van Lieshout, M. N. M. (2000). *Markov point processes and their applications* (p. 41). London: Imperial College Press.

Vega-García, C., Woodard, P. M., & Lee, B. S. (1993). Geographic and temporal factors that seem to explain human-caused fire occurrence in Whitecourt Forest, Alberta. In *GIS'93 Symposium*.

Warton, D. I., & Shepherd, L. C. (2010). Poisson point process models solve the "pseudo-absence problem" for presence-only data in ecology. *The Annals of Applied Statistics*, 4(3), 1383-1402.

Yang, J., He, H.S., Shifley, S.R., & Gustafson, E.J. (2007). Spatial patterns of modern period human-caused fire occurrence in the Missouri Ozark highlands. *Forest Science*, 53(1), 1-15.

Chapter 2. Assessing Fire Risk Using Monte Carlo Fire Spread Simulation

2.1 Introduction

Forest fire risk assessment is critical in allocating resources towards avoidance of potential devastation through sustainable forest management. As the magnitude and severity of fire escalates from changing climates, resulting in considerably higher costs per fire, it is becoming increasingly important to provide accurate information on fire risk (Liu et al., 2010). Following a longstanding drought starting in 2009, the Korean government has encouraged special countermeasures addressing prevention of forest fires (Korea Forest Service, 2011). These measures include enhancement of systems for fire surveillance and suppression, which aren't feasible without an adequate estimate of fire susceptibility and impact for a given area of interest.

The risk of forest fire is usually defined by two different components: fire behavior probability and fire effects (Finney, 2005). Fire behavior probability refers to the manner in which fire would burn a specific parcel of land (i.e. burn probability). It should be distinguished from fire occurrence probability, which denotes the relative frequency of ignition within an area. Fire behavior probability primarily addresses the propagation and intensity of an already ignited fire, while fire occurrence probability focuses on the environmental processes leading up to ignition. More specifically, the spread of fire is dependent on the ignition of fire as well as environmental conditions such as weather, topography, and fuels. This means that an estimate of fire ignition probability should precede an appraisal of the burn probability, and that fire ignition probability alone does not adequately surrogate fire behavior probability.

Due to their substantial uncertainty and variability, however, fire ignition probability and burn probability tend to be treated independently of one another (Thompson and Calkin, 2011).

The majority of fire spread models assume fixed ignition locations, which becomes a primary limitation of model applications in assessing potential fire risks for regions where fire ignition locations are uncertain. Some past studies have attempted to use empirical ignition locations or random ignition points for performing multiple fire spread simulations. In the Niokolo Koba National Park in Senegal, a set of randomly distributed fire sources were used in assessing risk of fire propagation in savanna ecosystems (Mbow et al., 2004). The burn probability in a wildland-urban interface (WUI) region in northwestern Wisconsin was obtained based on numerous individual fire spread simulations with random ignition locations (Bar Massada et al., 2009). Ager et al. (2007) extracted 1000 random ignition points to calculate burn probability in central Oregon to analyze wildfire risk to the northern spotted owl. Carmel et al. (2009) created 80% of ignition points within a vicinity of roads and small trails while 20% were chosen randomly within the study area in Mt. Carmel, Israel, based on the assumption that all forest fires in that region are anthropogenic. However, these studies do not adequately reflect a likelihood or spatial pattern of fire ignitions in their study regions. In this regard, Bar Massada et al (2009) pointed out that inappropriate ignition locations may potentially cause significant errors and biases in fire risk assessment. In research investigating influential factors of fire spread pattern, locations of forest fire ignition was the strongest and most direct variable affecting the area of fire spread (LaCroix et al., 2006). Unfortunately, little research has explored the concept of extracting ignition points based on a specific fire occurrence probability for fire spread simulations.

In this study, we attempted to form a link between burn probability and fire occurrence probability in order to derive fire behavior probability. The density of fire ignition points was modeled using a landscape in Gyeongju, Korea, using spatial point processing methods described in the previous chapter. We obtained a set of possible fire ignition locations from the model to

perform Monte Carlo fire spread simulations to calculate burn probability. We expect this connection between fire ignition and fire spread to provide more reliable risk assessments for forest fires. Details on our approach and results will follow in Section 2.2 and 2.3.

Obtaining a tangible set of expected fire ignition locations from an estimated fire occurrence probability model requires additional effort, as the majority of likelihood of fire occurrence outputs are expressed as a continuous and arbitrary population. The number of possible points is infinite and probability density functions fluctuate within each region. Methods for sampling discrete points from continuous and multi-dimensional distributions have been addressed using stochastic and mathematical methods in applied statistics. Spatial point processes adopt one of these procedures as a simulation process, allowing for easy realizations of the point pattern through Markov chain Monte Carlo (MCMC) simulation (Stoyan and Penttinen, 2000). We utilized the MCMC realizations of the point pattern as ignition locations of forest fires. In other words, fire spread simulation is constructed on the basis of ignition probability. Further details for the point pattern simulation process will be provided in section 2.2.

Vegetation, terrain, and weather conditions are critical determinants of both fire spread and fire behavior. In general, rates of fire spread accelerate with steepness of slope and high velocity of wind (Rothermel, 1972; Weise and Biging, 1997). Land cover, often referred to as a fuel model, is also a well-documented influence of fire spread (Anderson et al., 1982). Grass-dominated land cover is typically more prone to fire spread than forested areas, and dense forests burn more quickly than forests with wide dispersal of trees. Weather is one of the most critical elements manipulating fire behavior, both directly and indirectly. Temperature and humidity affect fuel moisture, while simultaneously interacting with each other. In addition, two or more environmental variables often collectively create different effects on fire spread. For example, Andrews (1986)

determined that the effect of wind speed on the rate of fire spread was an outcome of wind and slope combined. Likewise, fire behavior is also a consequence of intricate interactions among various factors, and can never be fully accounted for. Hence, it is common in fire spread simulation studies to treat temporally dependent variables, weather especially, as a fixed situation with the average extreme scenario (e.g., Bar Massada et al., 2009; LaCroix et al., 2006; Haas et al., 2014) due to convenience and more conservative risk assessment.

Advances in computational techniques have promoted development of a number of physical, empirical and mathematical fire behavior models and simulators, offering a broad range of options (for reviews, see Sullivan, 2009a~c). Implementations of geographical information systems (GIS) have also greatly simplified the process of fire simulations (Pastor et al., 2003). These fire simulation models are useful in providing practical and easily interpreted information for relevant authorities (Sullivan, 2009c). We employed FOREST FIRE SPREAD MODEL V4 (FFSM) developed by Lee et al. (2011) as the simulator to pursue this research, as the model is adapted and optimized to the study landscape. FFSM is a GIS-running fire spread calculation model applying Rothermel's equation (Rothermel, 1972) and the theory of elliptical wave propagation (Anderson et al., 1982). It is analogous to Farsite in the United States (Finney, 1994), Prometheus in Canada (Tymstra, 2002) and SiroFire in Australia (Coleman and Sullivan, 1995). As fire spread is greatly influenced by local environment, it is important to select a simulator that best describes the study landscape.

Fire effect indicates an expected outcome of a fire burn, both negative and positive (Finney, 2005). The outcome is often converted into economic, environmental, and social values, which diverge widely according to the stakeholders' interests. Mapping the pattern of fire behavior without considering resources of concern may provide less complete information about fire risks

(Thompson et al., 2011). Since these resources at risk have a vast range of applications, from housing and commercial timber to ecosystem services such as biodiversity and air quality (Ohlson et al., 2006), it is critical to be able to present reliable fire behavior estimations that can respond flexibly to various needs of stakeholders who may wish to deploy their own management strategies against fire.

The work we describe in this chapter adopted land property value as the fire effect to estimate potential loss for a given probability of fire spread, yet the value can be replaced by any others desired. By combining fire effect with an estimate of fire behavior probability based on fire occurrence probability we hope to consider the comprehensive elements of Finney's risk definition and provide an example of forest fire risk assessment. We expect to draw conclusions with respect to 1) how the burn probability is influenced by the environment across the region, 2) what is the spatial distribution of forest fire risk in the study area, and 3) which factor among the fire behavior probability and fire effect primarily contributes to the risk of forest fire.

2.2. Data and Method

2.2.1. Study area and data

The forested area within the administrative boundary of Gyeongju, Korea is the target study landscape for the fire spread simulation (Figure 2.1). For details on the study area, see chapter 1.4. To take the effect of terrain and land cover on the behavior of forest fires into account, a digital elevation model (DEM) and forest type map (fourth edition, Korea Forest Research Institute (2005)) were utilized as parameters describing topography and fuel models. The map of forest type contains digitized information on tree species composition, age, density, and diameter class,

allowing for consideration and control of vegetative influences on fire spread simulation. Both DEM and forest type map are set to default environments in the fire spread simulator FFSM V4.

Weather is regarded as the most influential factor on fire behavior (Prestemon et al., 2002). It is common in many fire simulation studies to assume an extreme weather scenario in order to anticipate the greatest risk (Finney, 2005; Bar Massada et al., 2009). In this study we configured a 95% extreme weather condition throughout the fire spread simulations. In Korea, the occurrence of forest fires is reported most frequently during the dry spring season (from April to May) according to the Statistical Yearbook of Forestry (Korea Forest Service, 2011). We therefore aggregated the records of daily weather in April and May from the past 5 years (i.e. from 2008 to 2012) from Yeongchun Weather Observatory located near the study landscape (Figure 2.1) and computed the 95th percentile extreme in temperature, relative humidity, and wind speed. Wind direction, which has a large impact on the direction of fire spread, was assumed to be the prevailing wind direction during the season. The weather scenario used for the simulation is summarized in Table 2.1. The weather condition was assumed to remain constant for duration of the fire.

For the purpose of providing an example of risk assessment, the government-appraised land property values were acquired from the municipal office of Gyeongju to serve as the fire effect. The data were spatially coded using the administrative parcel information number and then rasterized with 10-m resolution using ArcGIS 10.2 software (ESRI, 2012). Among a total of approximately 500,000 individual pieces of land included in the study landscape, about 110,000 parcels were analyzed in this study while the remaining land was excluded as non-forested lands (e.g., residential area) or unvalued parcels.

2.2.2. Derivation of fire ignition points: Metropolis-Hastings algorithm

Given the density of forest fire occurrence (Figure 1.13a) a possible suite of points is required to establish start locations of fire spread in simulation. In other words, we need one – or as many as necessary–sets of fire ignition points that form the same point density distribution as those modeled. Spatial point processes adopt a simulation method called the Metropolis-Hastings algorithm to realize a point pattern for a given density function (Geyer and Møller, 1994). The basic strategy of the M-H algorithm is to propose a trial distribution (i.e. proposal distribution) to randomly sample candidate points and accept or reject the candidate points with a probability proportional to the target distribution. If the acceptance (or rejection) of the candidate points occurs sequentially and iteratively (i.e. Markov Chain Monte Carlo simulation), the distribution of points eventually converges to the target density. The algorithm produces reliable samples even for an unnormalized density function (such as the Markov point process utilized in this study) using MCMC simulations (Illian et al., 2008). For details, see Geyer and Møller (1994).

In our case, the density function of the area-interaction model is expressed as;

$$f(x) = \alpha\beta^{n(x)}\gamma^{-|U_{x,r}|} \quad (1)$$

with a normalizing constant α and where β and γ denote the trend and interaction parameters respectively, shown in Table 1.4 in the previous chapter. This function is equivalent to the target distribution. Assuming that there is a set of points with a fixed number n ($x = \{x_1, x_2, \dots, x_n\}$) and a proposal distribution is given as $q(x,\cdot) > 0$, any randomly selected point x_i such that $i \in \{1, 2, \dots, n\}$ can be replaced with a candidate point, say y, which is randomly drawn from the proposal distribution $q_i(x, y)$. Whether the candidate point is accepted or rejected is determined with a probability of $\alpha_i(x, y) = \min\{1, r_i(x, y)\}$ such that

$$r_i(x, y) = \frac{f\big((x\backslash x_i) \cup y\big) q_i\big((x\backslash x_i) \cup y, x_i\big)}{f(x) q_i(x, y)}. \quad (2)$$

$r_i(x, y)$ is called the Hastings ratio and $\alpha_i(x, y)$ is referred to as acceptance probability. If the candidate is accepted, the current state is updated as $x' = (x \backslash x_i) \cup y = \{x_1, x_2, \dots, x_{i-1}, y, x_{i+1}, \dots, x_n\}$ and the next point x_m is selected to be replaced by y' with a probability of $\alpha_m(x', y')$ (i.e. Markov chain). With sufficient iterations of these processes (i.e. Monte Carlo simulation), the chain will typically converge to $f(x)$ regardless of the initial state x. Thus, the Hastings ratio denotes the probability density of proposing a move from x_i to x_m, and simultaneously assures the irreducibility and reversibility of the chain for any $f(x)$.

We demonstrated the M-H algorithm based on the density of forest fire ignition points presented above. The number of iterations was set at 100,000 with a 50,000 burn-in period (i.e. excising some prior chains as testing processes for enhancing reliability). Tracking the process of the algorithm is provided in Figure 2.2 at iterations 50,000, 70,000, 90,000, and 100,000. We obtained a point pattern and discarded points on non-target areas such as residential zones and incombustible areas (e.g., road surface and water body) regarding them as not being ignited. Consequently, a total of 502 points were extracted and converted into a vector containing (x, y)-coordinates representing ignition locations in fire spread simulations (Figure 2.1). The process of point pattern generation was conducted using the 'spatstat' package (Baddeley and Turner, 2006) in R software (R Development Core Team, 2010).

2.2.3. Fire spread simulation framework and fire risk assessment

FOREST FIRE SPREAD MODEL V4 (FFSM) developed by Lee (2011) was used to simulate the spread of individual fires across the landscape. FFSM is a vector-based simulation model defining fire propagation as an expanding polygon. The computation of fire spread in this simulator is based on Alexander's 2-dimensional elliptical shape of forest fire model (1985) and Richards' partial differential equation (1990). FFSM is a user-friendly tool that requires only a

few input data, including the locations of fire ignition points, weather parameters, terrain, and fuels (Figure 2.3).

In total, 502 fire simulations were conducted. Each simulation resulted in a unique fire spread pattern, stored in multiple polygons representing cumulative burn areas over a given fire duration. To analyze the effects of time on burn probability, four ascending time periods were established (e.g. 5, 10, 15, and 20 hours) during the full 20-hour fire duration. According to past data, 20 hours is the 95th percentile of time taken for fire suppression (Korea Forest Service, 2011). Consequences of fire spread from each ignition point were recorded separately, and sorted by corresponding time sequences. By overlaying all 502 individual fire spread results and averaging them, a burn probability (BP) for a specific time period in a given pixel was calculated as

$$BP\ (\%) = \frac{Number\ of\ burns}{Total\ number\ of\ simulations\ (502)} \times 100. \qquad (3)$$

We considered the fire effect to result in loss of land property values. Thus, the risk of forest fire is evaluated as the potential loss value for a given location in the following manner:

$$Land\ Property\ Value\ (per\ unit\ area) \times BP = Potential\ Value\ Loss. \qquad (4)$$

The obtained maps of BP for each time lag and the potential loss were then rasterized with 10-m resolution to visually describe spatial patterns of fire risks across the study landscape.

2.2.4. Statistical analysis of the risk-related factors

Four outputs regarding 1) fire ignition point density, 2) burn probability, 3) land price data, and 4) potential loss value map, are aligned to compute the covariance and correlation matrices for the purpose of investigating association of each risk element (i.e. fire probability, burn probability, and fire effect) with the resulting assessment. Pearson's correlation between any two factors is calculated as follows:

$$Corr_{ij} = \frac{Cov_{ij}}{\delta_i \delta_j} \quad (5)$$

where δ_i denotes the standard deviation of the ith pixel values and Cov_{ij} means the covariance between raster layers i and j $(i, j = 1, \dots, 4)$.

Table 2.1. The 95th percentile extreme weather condition used in fire spread simulation.

Temperature	Relative Humidity	Wind Speed	Wind Direction
16.3°	32.3%	4.2m/s	WNW

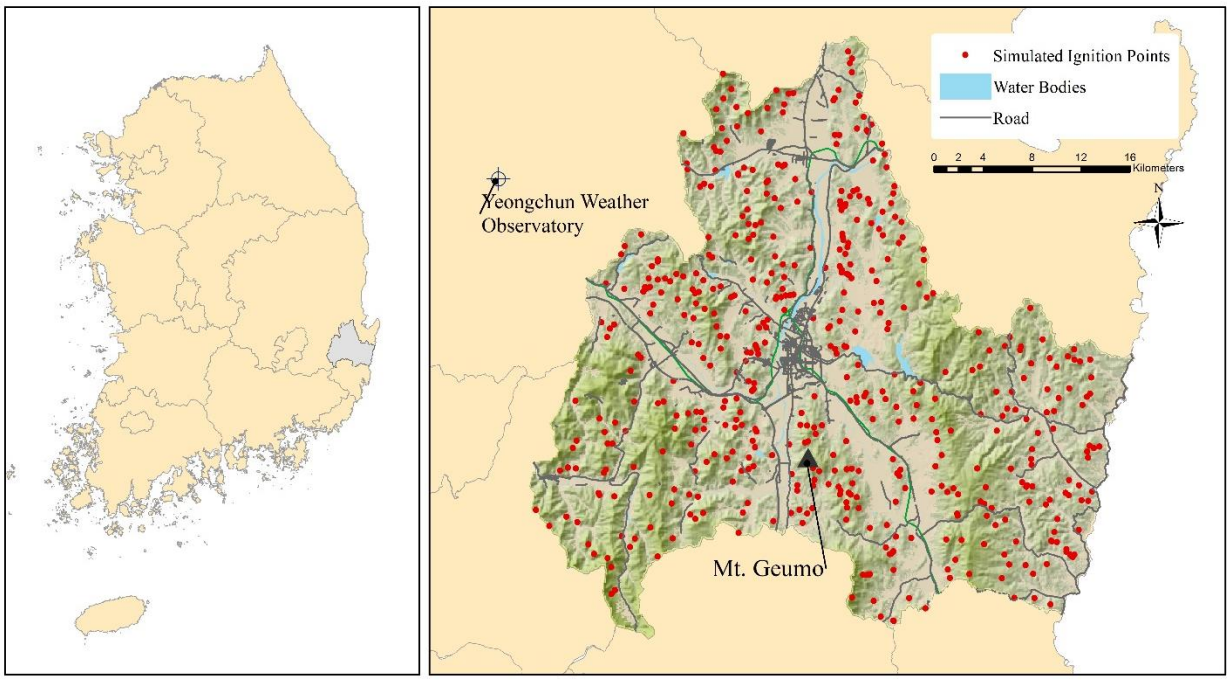

Figure 2.1. Locations of Yeongchun weather observatory (128.57.5°E. 35.58.38°N) and 502 ignition points derived from the estimated fire probability.

Figure 2.2. Realizations of point pattern using M-H algorithm under a given area-interaction model (constructed in the previous chapter). With 100,000 iterations and 50,000 burn-in iterations, the progress of the algorithm was tracked for the 50,000, 70,000, 90,000, and 100,000th iteration, respectively. A sub-total of 139 points are obtained as the first simulation set, and used as fire ignition points with three other sets of points obtained by the same algorithm setting. Some points distributed on noncombustible areas (e.g., residential area, water bodies, and etc.) were excluded during the fire spread simulation procedure, resulting in a total of 502 individual fire spread patterns.

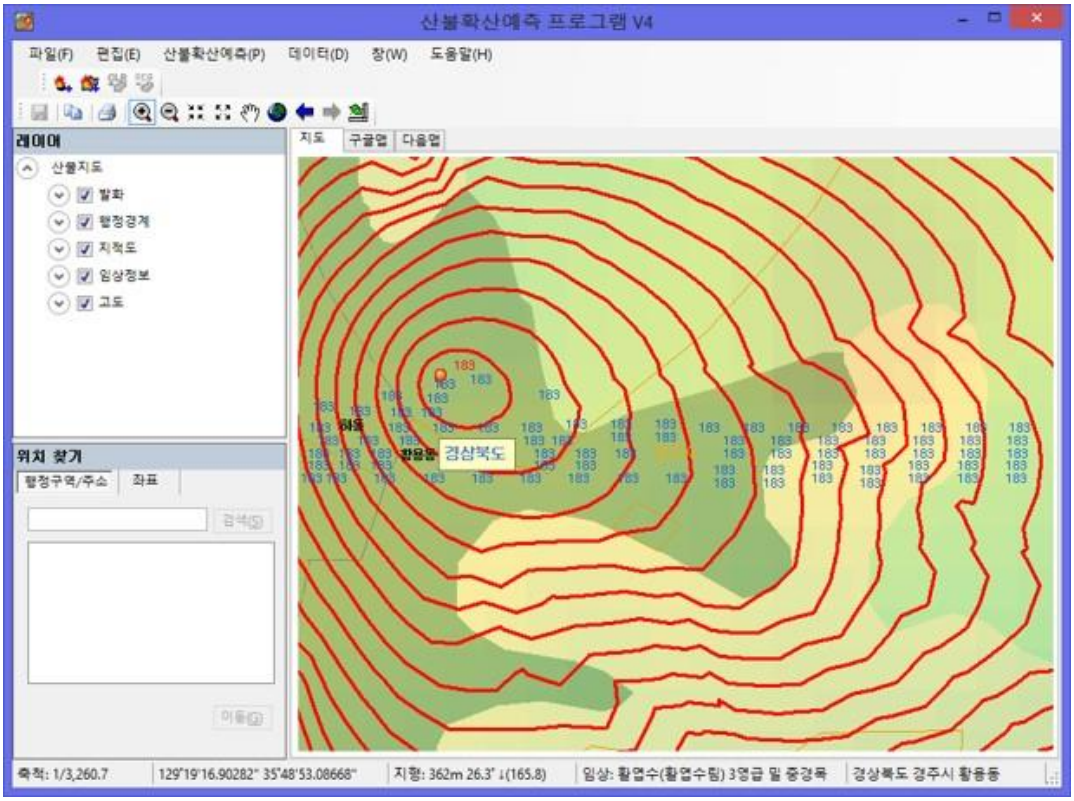

Figure 2.3. The control screen of fire spread simulator, FFSM.

2.3. Result and Discussion

2.3.1. Burn Probability Maps

The aggregation of 502 individual fire spread simulation results is presented in Figure 2.4 in order of time elapsed. Burn probability for overall fire durations ranged from 0 to approximately 7.6%, indicating that the highest frequency of burn on the same piece of area was 38 times out of 502 simulations under an extreme (95^{th} percentile) weather condition. When the fire lasted for 5 hours, about 52 hectares of forest were burned on average per fire. This is an extreme result considering that the average burn area is reported as only 2.7 ha per fire with 1 hour and 47 minutes of average suppression time (Korea Forest Service, 2011). Our simulation didn't account for fire extinction efforts, which, along with the extremity of weather used in simulation, contributed to our high estimate of area burned. As the duration of fire increases, the rate of spread in area (ha/hr)

also increases (Table 2.2). This can be attributed to the expansion of fire lines as fire duration increases, despite consistent fire spread rate in distance under the constant weather scenario. These results correspond well to previous research (Weber, 1989).

Examining the most extreme case of fire duration (i.e. 20 hours) (Figure 2.7), 74.9% of the entire area suffered from the spread of fire at least once during the simulation. The risk of forest fires under extreme conditions is classified into five successive stages (Table 2.3). The spatial distribution of burn probability in Gyeongju consists of mostly moderate level of risk (<2%) area. The relatively high risk area with the burn probability of 2~4% (i.e. 5 to 10 times of fire spread during 502 simulations) accounts for 2.37% of the entire region, and 0.96% of the region is at even higher risk. It is remarkable that the extreme rate (e.g. >6%, 30 or more times of fire spread during 502 simulation) of fire risk occupies up to 2.84% of the region, a percentage greater than for the 'High' and 'Very high' risks. This reveals that the risk of forest fire is spatially clustered at specific locations of the region.

The 'hot spots' containing high burn probabilities are mostly concentrated on the forest around Geumo-san and Gumi-san, the lower and upper center part of the study landscape (Figure 2.7). This is likely due to the close proximity of these forests to urbanized areas. According to the density of simulated ignition points (Figure 2.6), it appears that the distribution of burn probability is largely associated with high frequent fire occurrence areas. However, the forest around Geumo-san (marked in Figure 2.1) seems to have a relatively small number of fire occurrences in contrast to its excessively large burn frequencies, implying that burn probability may not be entirely dependent on the fire occurrence probability.

2.3.2. Risk assessment using land price data

The government-appraised land property value per unit area (m^2) of forested land in Gyeongju is presented in Figure 2.8. The lands with high value are primarily located in the center of the study landscape, in close proximity to urbanized areas, whereas the westernmost part of the landscape has relatively low values. As aforementioned, we considered land property loss from forest fire to describe the fire effect. This can be an example that presents relative risks in value among different locations of the landscape.

The final result of risk assessment, based on land property value combined with burn probability (with 20 hours of fire duration), shows fire risk as a function of fire effect and burn probability. Some areas with high fire risk potential shown in Figure 2.9 (i.e., orange to red colors) have either extremely high property values or extremely high burn probability. Although some areas have low property values (e.g., the area around Geumo-san), they appear to have relatively high fire loss because of their extreme burn probability (Figure 2.7). The circumstance where some areas with low property values have high fire risk due to a high burn probability suggests that fire risk is not dependent solely on either the burn probability or the fire effect.

2.3.3. Factors affecting the risk of forest fire

Pearson's correlations among the fire probability, burn probability, land price, and expected loss are provided in Table 2.4. Note that the variables used for correlation calculation are log-transformed. The expected loss value showed the highest correlation rate ($r = 0.7084$) with the burn probability, followed by the land price data ($r = 0.4169$) and the fire probability ($r = 0.3969$). This result indicates that the amount of loss from forest fires is largely affected by the burn probability, and the effect of actual property values is relatively subsidiary. It also implies that the burn probability calculated as a combination of fire ignition and fire spread provides more precise information than the ignition probability alone in assessing risk of forest fire. The burn

probability shows a considerable correlation with the density of ignition points ($r = 0.3960$) but not exclusively, implying that the pattern of fire spread is influenced by the fire occurrences to some extent (i.e. weak to moderate), but are separate processes. Meanwhile, the spatial distribution of land price has little connection with the fire probability ($r = 0.1323$) or burn probability ($r = 0.0240$).

2.3.4. Further approach

In this study, government-appraised land property values were utilized as the value of loss from forest fires, but other loss values such as potential resource damages, environmental and social values can be easily incorporated with our approach. Fire may influence land property values (Donovan et al., 2007; Mueller et al., 2009), but the entirety of the land value would not be lost from fire. It thus may not be appropriate to assess fire risks based on land values. In application, the amount of government compensation for property damage from forest fire can be based on the value of forest stock. However, estimates of loss to forest stock cannot completely represent injury either, since it does not fully address all of the other economic, ecological, and social losses involved. Future research should address and quantify potential fire losses that are sensitive to location, fire severity, land use, population, and other ecological and social values in order to better reflect the real costs of forest fires.

Weather is one of the primary factors influencing fire behavior, both directly and indirectly by affecting fuel condition and availability (Bessie and Johnson, 1995). Microclimate is subject to change minute by minute, complicating prediction of fire spread. In this study, weather was assumed to remain constant during the fire duration for simplicity of simulation. Even though this assumption is not uncommon in many simulation studies (e.g., Stephens, 1998; Mbow et al., 2004; Schmidt et al., 2008), it may cause bias –usually toward overestimation –in fire spread prediction.

Previous research has made attempts to diversify weather scenarios by averaging temperature and humidity of each month and distributing fire ignitions among monthly fire occurrence rates (e.g. Bar Massada et al., 2009), or by using climate records of randomly selected date (Carmel et al., 2009). Consideration of weather variance in analyzing fire behavior (e.g., using wind field or remotely sensed data) would allow more realistic fire risk assessment. However, such considerations inevitably demand more capacity for computational time and load, and add layers of complexity to an already complex fire spread simulation process.

Table 2.2. Parameters of burn area resulted from fire spread simulations for each level of fire duration.

Fire Duration (hour)	Mean Area (ha)	Min. Area (ha)	Max. Area (ha)	S.D. (ha)	Rate of Spread in Area (ha/hr)
5	51.9749	0.7505	259.0731	36.8299	10.3950
10	170.0403	0.8206	902.4563	124.7508	34.0081
15	329.0854	0.8206	1644.9086	243.1726	65.8171
20	514.6184	0.8206	2402.8163	380.6499	102.9237

Table 2.3. Classification of fire risk according to the range of estimated burn probability.

Fire Risk	Range of Burn Probability	Percentage to Total (%)
Low	0%	25.10
Moderate	0~2%	68.72
High	2~4%	2.37
Very high	4~6%	0.96
Extreme	>6%	2.84

Table 2.4. Pearson's correlation between the log-transformed values of resulted raster layers.

	Fire Probability	Burn Probability	Land Price	Expected Loss Value
Fire Probability	1			
Burn Probability	0.3960	1		
Land Price	0.1323	0.0239	1	
Expected Loss Value	0.3969	0.7084	0.4169	1

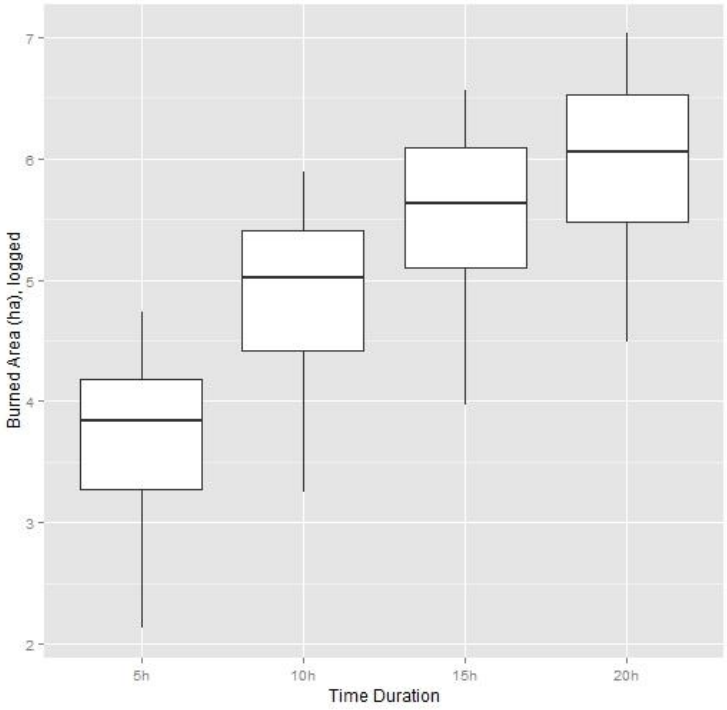

Figure 2.4. Simulated mean, maximum, and minimum burned area corresponding to fire duration. Note that the 10% of data were trimmed from each time duration to exclude extreme cases. The scale of y-axis is logarithmic.

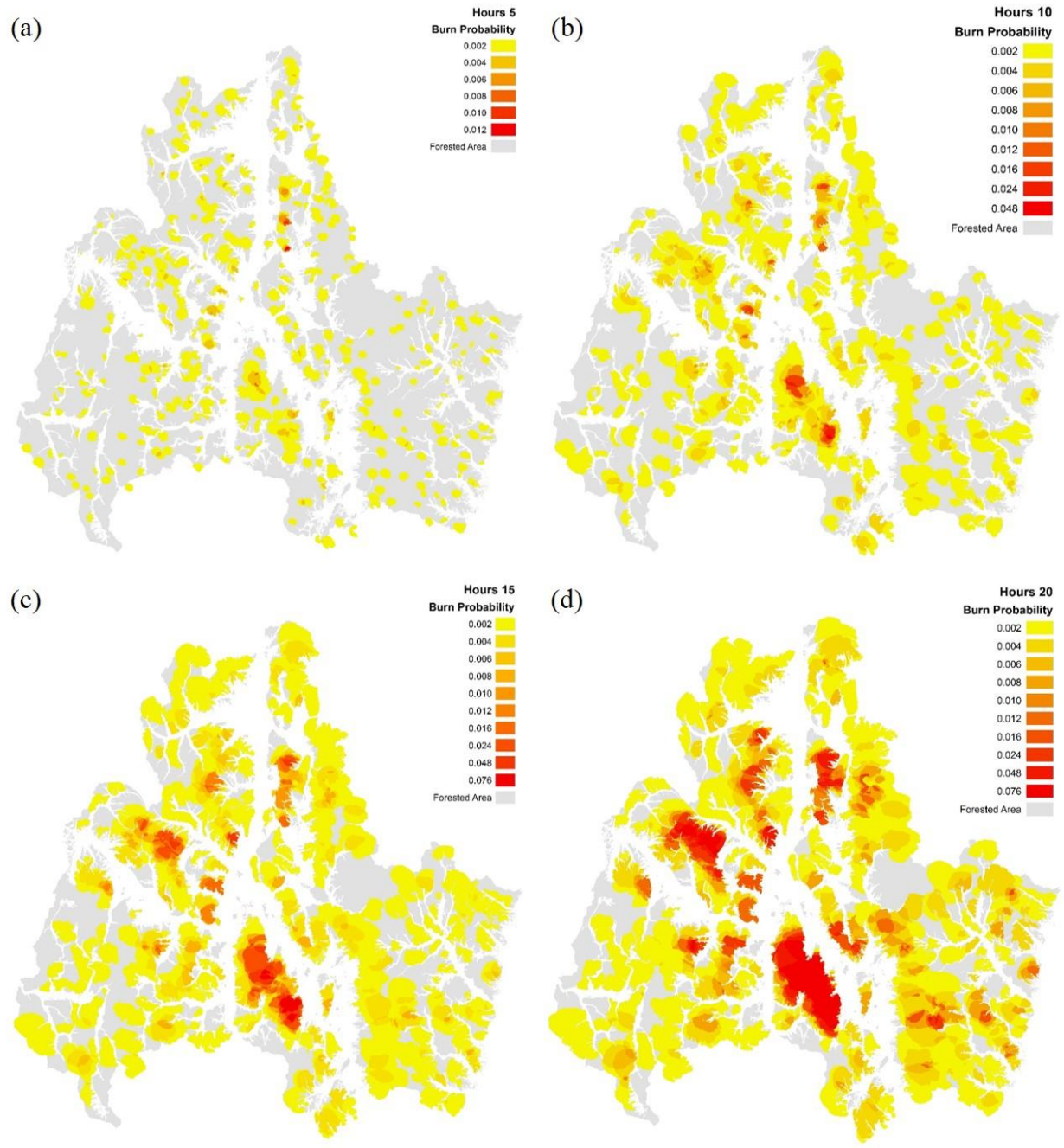

Figure 2.5. Spatial distributions of burn probability estimated from 500 fire spread simulations for the duration of (a) 5 hours, (b) 10 hours, (c) 15 hours, and (d) 20 hours.

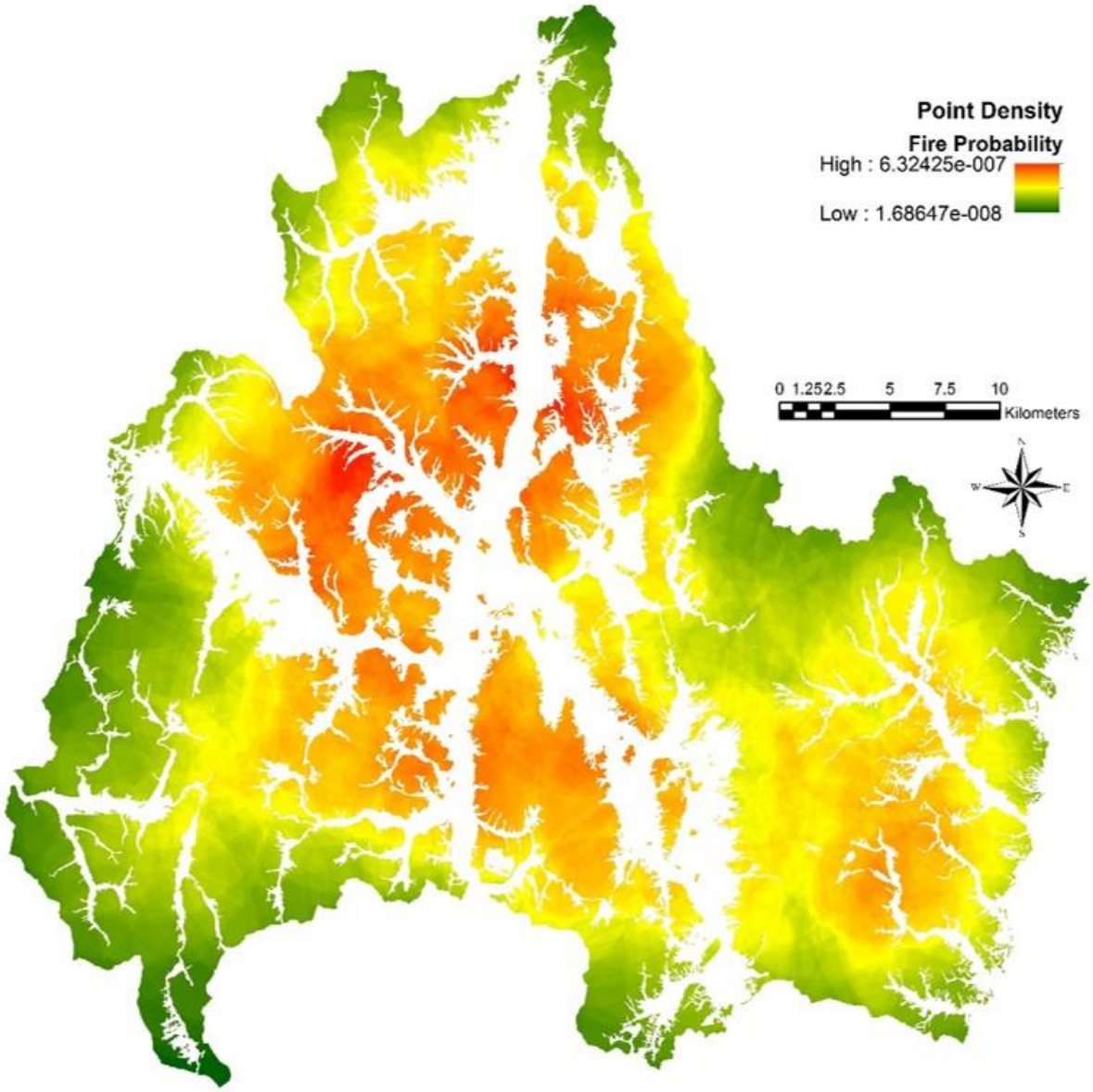

Figure 2.6. Estimated density of forest fire ignition points (i.e. fire probability) in Gyeongju, Korea.

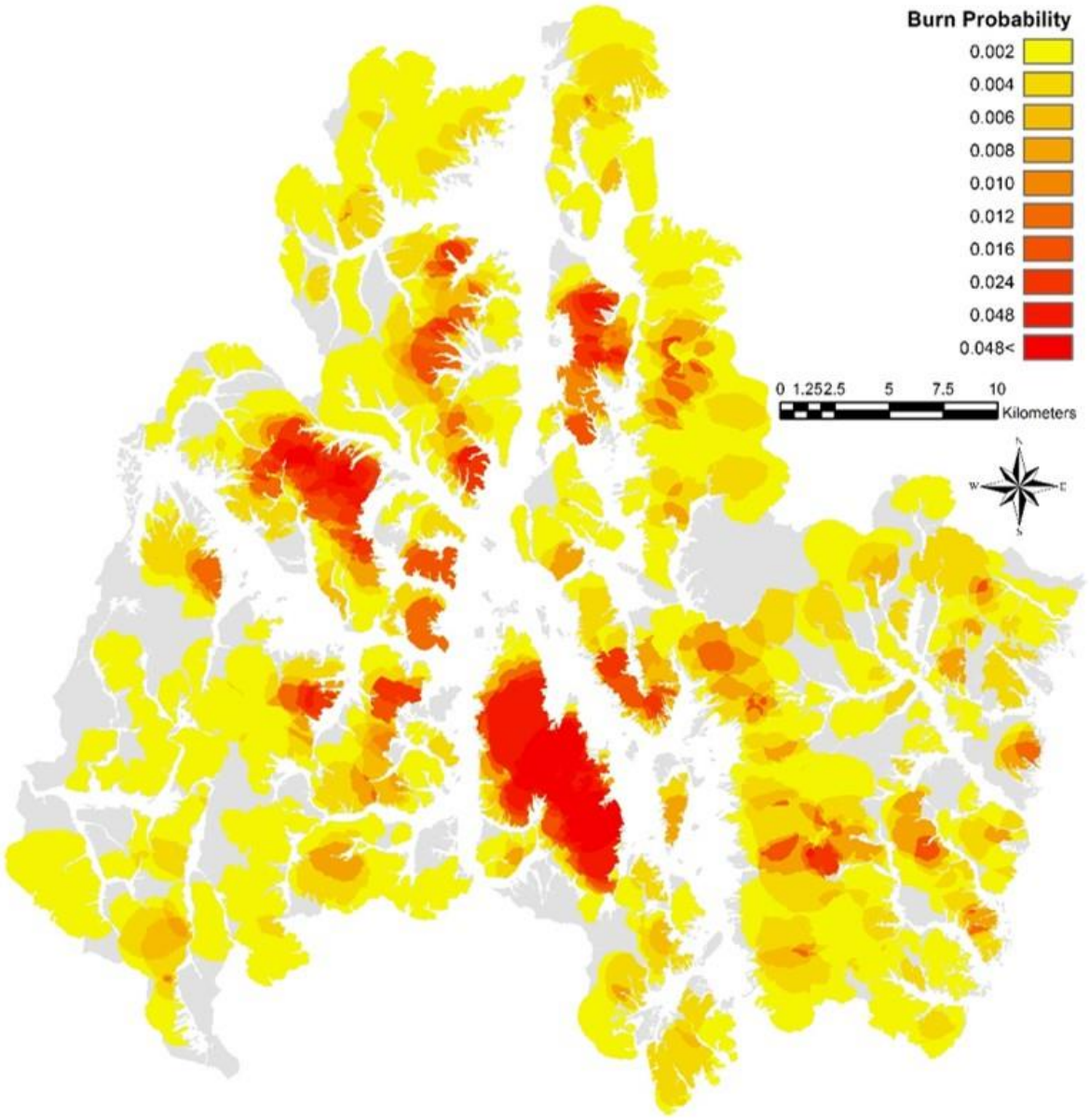

Figure 2.7. Estimated burn probability in Gyeongju, Korea.

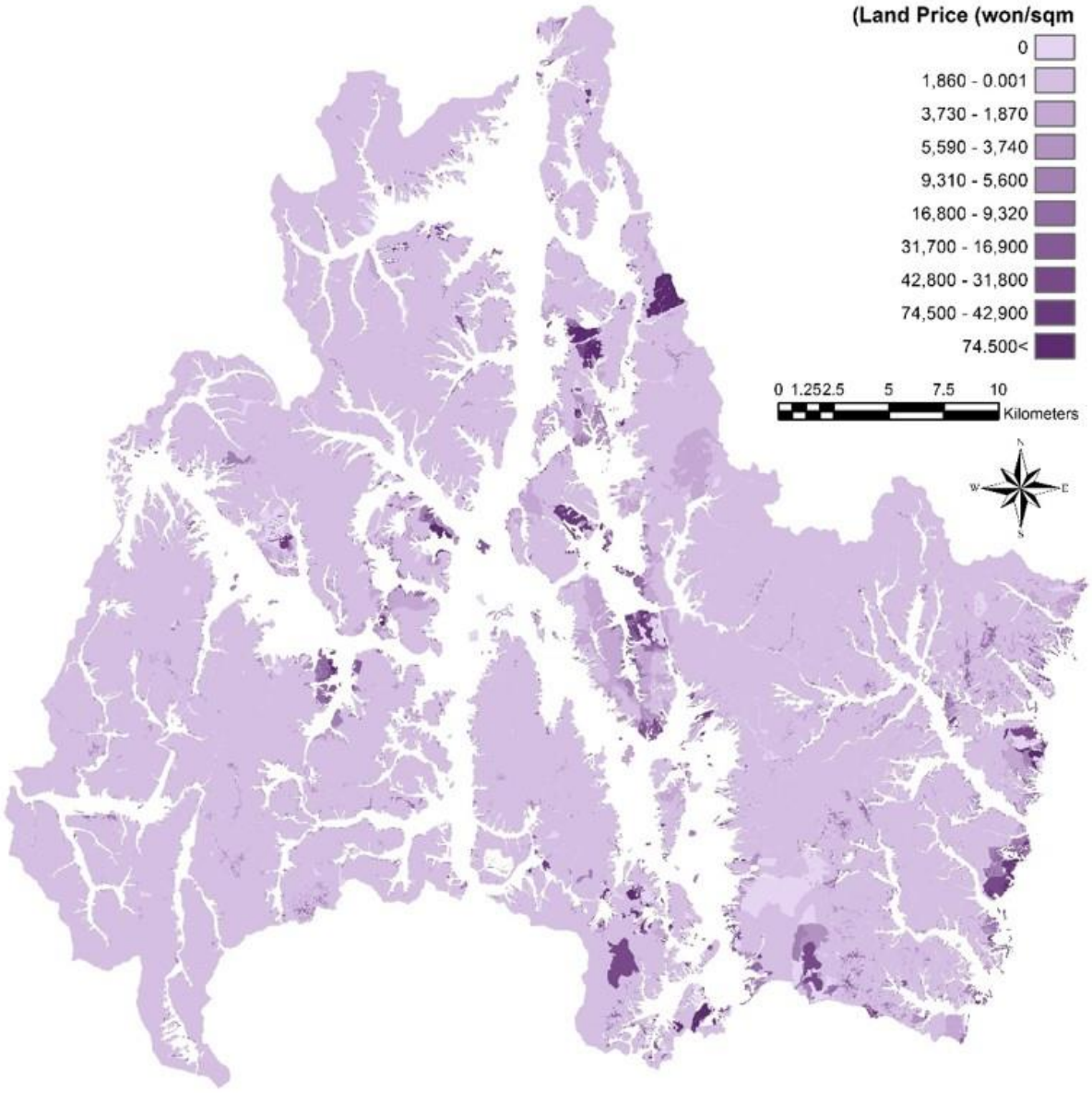

Figure 2.8. Spatial distribution of land property value in Gyeongju, Korea.

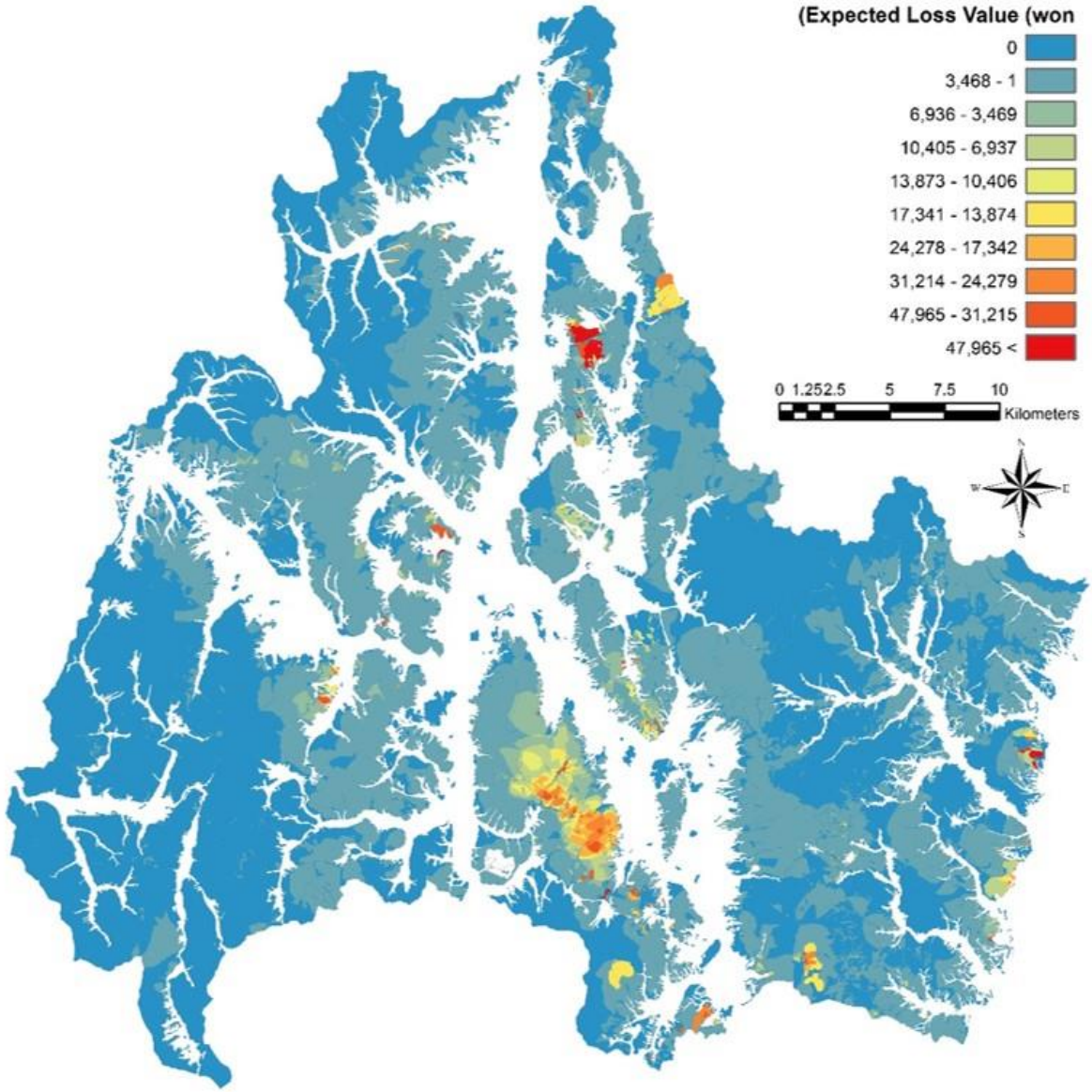

Figure 2.9. Potential fire loss estimated from the burn probability and land property values.

2.4. Conclusion

This study assessed risk of forest fires in Gyeongju, Republic of Korea based on Finney's definition of wildfire risk (Finney, 2005). Fire behavior probability in each land parcel across the landscape was estimated using Monte Carlo fire spread simulation that considered fire ignition locations, topography, land cover, and a 95th percentile weather condition. A suite of fire ignition locations were derived from the fire ignition point density model described in the previous chapter. Fire effect was included in the form of land property value, which can be substituted by any other variables of concern depending on stakeholder's interest. Forest fire risk assessed as a product of burn probability and property value, has a higher association with burn probability than land property value. Burn probability was related to the fire ignition point density to some extent, but not dominated by it. These findings support our initial speculation that fire behavior probability differs from fire occurrence probability, and both elements of forest fires should be considered in assessing the full spectrum of fire risk.

Incorporation of fire occurrence potential into burn probability estimation seems logical and necessary, yet a direct comparison is not made in this study between burn probability with and without fire occurrence potential considered. Quantifying the effects of fire occurrence consideration on burn probability estimation and a comparison with the effects of random ignitions would be warranted in future studies.

2.5 References

Ager, A. A., Finney, M. A., Kerns, B. K., & Maffei, H. (2007). Modeling wildfire risk to northern spotted owl (*Strix occidentalis* caurina) habitat in Central Oregon, USA. *Forest Ecology and Management*, 246(1), 45-56.

Alexander, M. E. (1985, April). Estimating the length-to-breadth ratio of elliptical forest fire patterns. In *Proc. 8th Conf. Fire and Forest Meteorology* (pp. 287-304).

Anderson, D. H., Catchpole, E. A., De Mestre, N. J., & Parkes, T. (1982). Modelling the spread of grass fires. *Journal of the Australian Mathematical Society*, 23, 451-466.

Andrews, P. L. (1986). BEHAVE: fire behavior prediction and fuel modeling system-BURN subsystem, Part 1.

Baddeley, A., & Turner, R. (2006). Modelling spatial point patterns in R. In *Case studies in spatial point process modeling* (pp. 23-74). Springer New York.

Ball, G. L., & Guertin, D. P. (1992). Improved fire growth modeling. *International Journal of Wildland Fire*, 2(2), 47-54.

Bar Massada, A., Radeloff, V. C., Stewart, S. I., & Hawbaker, T. J. (2009). Wildfire risk in the wildland–urban interface: a simulation study in northwestern Wisconsin. *Forest Ecology and Management*, 258(9), 1990-1999.

Bessie, W. C., & Johnson, E. A. (1995). The relative importance of fuels and weather on fire behavior in subalpine forests. *Ecology*, 76(3), 747-762.

Carmel, Y., Paz, S., Jahashan, F., & Shoshany, M. (2009). Assessing fire risk using Monte Carlo simulations of fire spread. *Forest Ecology and Management*, 257(1), 370-377.

Coleman, J., & Sullivan, A. (1995). SiroFire. the CSIRO Bushfire Spread Simulator. Proc Inst Forest Aust 16th Biennial Conf, Canberra.

Donovan, G. H., Champ, P. A., & Butry, D. T. (2007). Wildfire risk and housing prices: a case study from Colorado Springs. *Land Economics*, 83(2), 217-233.

ESRI 2012. ArcGIS Desktop: Release 10.2. Redlands, CA: Environmental Systems Research Institute.

Finney, M. A. (1994, October). Modeling the spread and behavior of prescribed natural fires. In *Proceedings of the 12th Conference on Fire and Forest Meteorology* (pp. 138-143).

Finney, M. A. (2005). The challenge of quantitative risk analysis for wildland fire. *Forest Ecology and Management*, 211(1), 97-108.

Geyer, C. J., & Møller, J. (1994). Simulation procedures and likelihood inference for spatial point processes. *Scandinavian Journal of Statistics*, 359-373.

Haas, J. R., Calkin, D. E., & Thompson, M. P. (2014). Wildfire risk transmission in the Colorado Front Range, USA. *Risk analysis*.

Illian, J., Penttinen, A., Stoyan, H., & Stoyan, D. (2008). *Statistical analysis and modelling of spatial point patterns* (Vol. 70). John Wiley & Sons.

Korea Forest Service. (2011). *Statistical Yearbook of Forestry 2011*, Daejeon, Republic of Korea

LaCroix, J. J., Ryu, S. R., Zheng, D., & Chen, J. (2006). Simulating fire spread with landscape management scenarios. *Forest Science*, 52(5), 522-529.

Lee, B. D., Lee, Y. H., Lee, M. B., & Albers, H. J. (2011). Stochastic Simulation Model of Fire Occurrence in the Republic of Korea. *Journal of Korean Forestry Society*.

Liu, Y., Stanturf, J., & Goodrick, S. (2010). Trends in global wildfire potential in a changing climate. *Forest Ecology and Management*, 259(4), 685-697.

Mbow, C., Goïta, K., & Bénié, G. B. (2004). Spectral indices and fire behavior simulation for fire risk assessment in savanna ecosystems. *Remote Sensing of Environment*, 91(1), 1-13.

Miller, C., Landres, P. B., & Alaback, P. B. (1999, June). Evaluating risks and benefits of wildland fire at landscape scales. In *Proceedings of the Joint Fire Science Conference and Workshop:"Crossing the Millennium: Integrating Spatial Technologies and Ecological Principles for a New Age in Fire Management," Boise, Idaho* (pp. 78-87).

Mueller, J., Loomis, J., & González-Cabán, A. (2009). Do repeated wildfires change homebuyers' demand for homes in high-risk areas? A hedonic analysis of the short and long-term effects of repeated wildfires on house prices in Southern California. *The Journal of Real Estate Finance and Economics*, 38(2), 155-172.

Ohlson, D. W., Berry, T. M., Gray, R. W., Blackwell, B. A., & Hawkes, B. C. (2006). Multi-attribute evaluation of landscape-level fuel management to reduce wildfire risk. *Forest Policy and Economics*, 8(8), 824-837.

Pastor, E., Zarate, L., Planas, E., & Arnaldos, J. (2003). Mathematical models and calculation systems for the study of wildland fire behaviour. *Progress in Energy and Combustion Science*, 29(2), 139-153.

Prestemon, J. P., Pye, J. M., Butry, D. T., Holmes, T. P., & Mercer, D. E. (2002). Understanding broadscale wildfire risks in a human-dominated landscape. *Forest Science*, 48(4), 685-693.

R Development Core Team. (2010). R software.

Richards, G. D. (1990). An elliptical growth model of forest fire fronts and its numerical solution. *International Journal for Numerical Methods in Engineering*, 30(6), 1163-1179.

Rothermel, R. C. (1972). A mathematical model for predicting fire spread in wildland fuels.

Schmidt, D. A., Taylor, A. H., & Skinner, C. N. (2008). The influence of fuels treatment and landscape arrangement on simulated fire behavior, Southern Cascade range, California. *Forest Ecology and Management*, 255(8), 3170-3184.

Stephens, S. L. (1998). Evaluation of the effects of silvicultural and fuels treatments on potential fire behaviour in Sierra Nevada mixed-conifer forests. *Forest Ecology and Management*, 105(1), 21-35.

Stoyan, D., & Penttinen, A. (2000). Recent applications of point process methods in forestry statistics. *Statistical Science*, 61-78.

Sullivan, A. L. (2009a). Wildland surface fire spread modelling, 1990–2007. 1: Physical and quasi-physical models. *International Journal of Wildland Fire*, 18(4), 349-368.

Sullivan, A. L. (2009b). Wildland surface fire spread modelling, 1990–2007. 2: Empirical and quasi-empirical models. *International Journal of Wildland Fire*, 18(4), 369-386.

Sullivan, A. L. (2009c). Wildland surface fire spread modelling, 1990–2007. 3: Simulation and mathematical analogue models. *International Journal of Wildland Fire*, 18(4), 387-403.

Thompson, M. P., & Calkin, D. E. (2011). Uncertainty and risk in wildland fire management: a review. *Journal of Environmental Management*, 92(8), 1895-1909.

Thompson, M. P., Calkin, D. E., Finney, M. A., Ager, A. A., & Gilbertson-Day, J. W. (2011). Integrated national-scale assessment of wildfire risk to human and ecological values. *Stochastic Environmental Research and Risk Assessment*, 25(6), 761-780.

Tymstra, C. (2002). PROMETHEUS—the Canadian wildland fire growth model. *Initial Attack*, 2002, 8-9.

Wallace, G. (1993). A numerical fire simulation-model. *International Journal of Wildland Fire*, 3(2), 111-116.

Weber, R. O. (1989). Analytical models for fire spread due to radiation. *Combustion and flame*, 78(3), 398-408.

Weise, D. R., & Biging, G. S. (1997). A qualitative comparison of fire spread models incorporating wind and slope effects. *Forest Science*, 43(2), 170-180.

Concluding Remarks

Forest fire is a complicated event affected by multiple factors and their interactions. Because of the complexity, most previous studies dealt with exclusively either fire occurrence potential or burn probability to assess fire risks. This research attempted to incorporate fire occurrence potential into burn probability estimation, while exploring a new approach to model fire ignition locations using point patterns in SPP modeling. The resulted burn probability map appears to successfully involve fire occurrence probability in a statistically rational way (e.g. M-H algorithm), and can be combined with any measure of loss that is of importance to stakeholders (e.g. forest stocks, structures, social and cultural value of properties).

Both occurrence and behavior of forest fires are riddled with uncertainty, and a myriad of errors may exist in predicting them, not only during each of stages but also as a colligated process. Errors may originate from statistical methodology of modeling, performance of the simulator, or even measurement of data. In addition, there would be a bias in assessing forest fire risk if both occurrence and behavior of fire are not considered simultaneously. This research was aimed to reduce such bias by combining modeled fire ignition density with fire spread simulations.

The presented study suggested implementations of SPP as an intuitive way for estimating fire occurrence probabilities. With the model performance which is similar or better than conventional logistic model, SPP could be a good alternative method to solve a pseudo-absence problem in estimating fire occurrence probability. If a numerical evidence of better performance of SPP models compared to conventional logit models is available (e.g., pseudo-likelihood for both Poisson and non-Poisson models), the use of SPP would be more justifiable.

Future studies should build on this study to improve the current limitations. Incorporation of microclimate variation would result in more realistic fire behavior probability modeling.

Addressing temporal effects on changes in burn probability due to vegetation growth and forest management activities over time could provide another piece of important information that would be useful for forest landscape management. Incorporating various economic, environmental, and social fire effects could provide better representations of fire risks.

Despite several limitations previously mentioned, our modeling approach has the ability to generate spatial distribution of fire occurrence, burn probability and potential fire loss, and can provide useful information for forest planning and resource allocation in fire management and suppression. Effective decision-making on allocation of finite resources for fire management requires a quality estimation on high-risk areas and their values at risk. With further improvement, we hope that our approach can serve this purpose.

BIBLIOGRAPHY

Ager, A. A., Finney, M. A., Kerns, B. K., & Maffei, H. (2007). Modeling wildfire risk to northern spotted owl (*Strix occidentalis* caurina) habitat in Central Oregon, USA. *Forest Ecology and Management*, 246(1), 45-56.

Akaike, H. (1974). A new look at the statistical model identification. *Automatic Control, IEEE Transactions on*, 19(6), 716-723.

Alexander, M. E. (1985, April). Estimating the length-to-breadth ratio of elliptical forest fire patterns. In *Proc. 8th Conf. Fire and Forest Meteorology* (pp. 287-304).

Anderson, D. H., Catchpole, E. A., De Mestre, N. J., & Parkes, T. (1982). Modelling the spread of grass fires. *Journal of the Australian Mathematical Society*, 23, 451-466.

Andrews, P. L. (1986). BEHAVE: fire behavior prediction and fuel modeling system-BURN subsystem, Part 1.

Baddeley, A. J., Møller, J., & Waagepetersen, R. (2000). Non-and semi-parametric estimation of interaction in inhomogeneous point patterns. *Statistica Neerlandica*, 54(3), 329-350.

Baddeley, A. J., & Turner, R. (2004). Spatstat: An R Package for Analyzing Spatial Point Pattens.

Baddeley, A. J., & Van Lieshout, M. N. M. (1995). Area-interaction point processes. *Annals of the Institute of Statistical Mathematics*, 47(4), 601-619.

Baddeley, A., & Turner, R. (2000). Practical maximum pseudolikelihood for spatial point patterns. *Australian & New Zealand Journal of Statistics*, 42(3), 283-322.

Baddeley, A., & Turner, R. (2006). Modelling spatial point patterns in R. In *Case studies in spatial point process modeling* (pp. 23-74). Springer New York.

Baddeley, A., Turner, R., Møller, J., & Hazelton, M. (2004). Residual analysis for spatial point processes. *AMS Clasification*.

Ball, G. L., & Guertin, D. P. (1992). Improved fire growth modeling. *International Journal of Wildland Fire*, 2(2), 47-54.

Bar Massada, A., Radeloff, V. C., Stewart, S. I., & Hawbaker, T. J. (2009). Wildfire risk in the wildland–urban interface: a simulation study in northwestern Wisconsin. *Forest Ecology and Management*, 258(9), 1990-1999.

Berman, M., & Turner, T. R. (1992). Approximating point process likelihoods with GLIM. *Applied Statistics*, 31-38.

Besag, J. E. (1977). Comments on Ripley's paper. *Journal of the Royal Statistical Society B*, 39(2), 193-195.

Besag, J., Milne, R., & Zachary, S. (1982). Point process limits of lattice processes. *Journal of Applied Probability*, 210-216.

Bessie, W. C., & Johnson, E. A. (1995). The relative importance of fuels and weather on fire behavior in subalpine forests. *Ecology*, 76(3), 747-762.

Bozdogan, H. (1987). Model selection and Akaike's information criterion (AIC): The general theory and its analytical extensions. *Psychometrika*, 52(3), 345-370.

Bradley, A. F., Noste, N. V., & Fischer, W. C. (1992). Fire ecology of forests and woodlands in Utah.

Calkin, D. E., Cohen, J. D., Finney, M. A., & Thompson, M. P. (2014). How risk management can prevent future wildfire disasters in the wildland-urban interface. Proceedings of the National Academy of Sciences, 111(2), 746-751.

Cardille, J. A., Ventura, S. J., & Turner, M. G. (2001). Environmental and social factors influencing wildfires in the Upper Midwest, United States. *Ecological Applications*, 11(1), 111-127.

Carmel, Y., Paz, S., Jahashan, F., & Shoshany, M. (2009). Assessing fire risk using Monte Carlo simulations of fire spread. *Forest Ecology and Management*, 257(1), 370-377.

Catry, F. X., Rego, F. C., Bação, F. L., & Moreira, F. (2010). Modeling and mapping wildfire ignition risk in Portugal. *International Journal of Wildland Fire*, 18(8), 921-931.

Chou, Y. H., Minnich, R. A., & Chase, R. A. (1993). Mapping probability of fire occurrence in San Jacinto Mountains, California, USA. *Environmental Management*, 17(1), 129-140.

Coleman, J., & Sullivan, A. (1995). SiroFire. the CSIRO Bushfire Spread Simulator. Proc Inst Forest Aust 16th Biennial Conf, Canberra.

Cox, D. R., & Isham, V. (1980). *Point processes* (Vol. 12). CRC Press.

Diggle, P. J. (1983). *Statistical analysis of spatial point patterns*. Academic Press.

Donovan, G. H., Champ, P. A., & Butry, D. T. (2007). Wildfire risk and housing prices: a case study from Colorado Springs. *Land Economics*, 83(2), 217-233.

ESRI 2012. ArcGIS Desktop: Release 10.2. Redlands, CA: Environmental Systems Research Institute.

Finney, M. A. (1994). Modeling the spread and behavior of prescribed natural fires. In *Proceedings of the 12th Conference on Fire and Forest Meteorology* (pp. 138-143).

Finney, M. A. (2005). The challenge of quantitative risk analysis for wildland fire. *Forest Ecology and Management*, 211(1), 97-108.

Garcia, C. V., Woodard, P. M., Titus, S. J., Adamowicz, W. L., & Lee, B. S. (1995). A logit model for predicting the daily occurrence of human caused forest-fires. *International Journal of Wildland Fire*, 5(2), 101-111.

Genton, Marc G.; Butry, David T.; Gumpertz, Marcia L.; Prestemon, Jeffrey P. (2006). Spatio-temporal analysis of wildfire ignitions in the St. Johns River Water Management District, Florida. *International Journal of Wildland Fire*. 15: 87-97.

Geyer, C. J., & Møller, J. (1994). Simulation procedures and likelihood inference for spatial point processes. *Scandinavian Journal of Statistics*, 359-373.

Haas, J. R., Calkin, D. E., & Thompson, M. P. (2014). Wildfire risk transmission in the Colorado Front Range, USA. *Risk analysis*.

Hering, A. S., Bell, C. L., & Genton, M. G. (2009). Modeling spatio-temporal wildfire ignition point patterns. *Environmental and Ecological Statistics*, 16(2), 225-250.

Huang, F., & Ogata, Y. (2002). Generalized pseudo-likelihood estimates for Markov random fields on lattice. *Annals of the Institute of Statistical Mathematics*, 54(1), 1-18.

Illian, J., Penttinen, A., Stoyan, H., & Stoyan, D. (2008). *Statistical analysis and modelling of spatial point patterns* (Vol. 70). John Wiley & Sons.

Juan, P., Mateu, J., & Saez, M. (2012). Pinpointing spatio-temporal interactions in wildfire patterns. *Stochastic Environmental Research and Risk Assessment*, 26(8), 1131-1150.

Kelly, F. P., & Ripley, B. D. (1976). A note on Strauss's model for clustering. *Biometrika*, 357-360.

Korea Forest Service. (2011). *Statistical Yearbook of Forestry 2011*, Daejeon, Republic of Korea

Korea Forest Service. (2012). *Statistical Yearbook of Forestry 2012*, Daejeon, Republic of Korea

LaCroix, J. J., Ryu, S. R., Zheng, D., & Chen, J. (2006). Simulating fire spread with landscape management scenarios. *Forest Science*, 52(5), 522-529.

Law, R., Illian, J., Burslem, D. F., Gratzer, G., Gunatilleke, C. V. S., & Gunatilleke, I. A. U. N. (2009). Ecological information from spatial patterns of plants: insights from point process theory. *Journal of Ecology*, 97(4), 616-628.

Lee, B. D., Lee, Y. H., Lee, M. B., & Albers, H. J. (2011). Stochastic Simulation Model of Fire Occurrence in the Republic of Korea. *Journal of Korean Forestry Society*.

Lee, B., Park, P. S., & Chung, J. (2006). Temporal and spatial characteristics of forest fires in South Korea between 1970 and 2003. *International Journal of Wildland Fire*, 15(3), 389-396.

Legendre, P. (1993). Spatial autocorrelation: trouble or new paradigm?. *Ecology*, 74(6), 1659-1673.

Liu, Y., Stanturf, J., & Goodrick, S. (2010). Trends in global wildfire potential in a changing climate. *Forest Ecology and Management*, 259(4), 685-697.

Lloyd, O. L., Smith, G., Lloyd, M. M., Holland, Y., & Gailey, F. (1985). Raised mortality from lung cancer and high sex ratios of births associated with industrial pollution. *British journal of industrial medicine*, 42(7), 475-480.

Mbow, C., Goïta, K., & Bénié, G. B. (2004). Spectral indices and fire behavior simulation for fire risk assessment in savanna ecosystems. *Remote Sensing of Environment*, 91(1), 1-13.

McCaffrey, S. (2006). What does "wildfire risk" mean to the public. The Public and Wildland Fire Management: Social Science Findings for Managers. General Technical Report NRS-1.

Newton Square, PA: US Department of Agriculture, Forest Service, Northern Research Station, 33-45.

McCaffrey, S., Toman, E., Stidham, M., & Shindler, B. (2013). Social science research related to wildfire management: an overview of recent findings and future research needs. International Journal of Wildland Fire, 22(1), 15-24.

Mercer, D. E., & Prestemon, J. P. (2005). Comparing production function models for wildfire risk analysis in the wildland–urban interface. *Forest Policy and Economics*, 7(5), 782-795.

Miller, C., Landres, P. B., & Alaback, P. B. (1999, June). Evaluating risks and benefits of wildland fire at landscape scales. In *Proceedings of the Joint Fire Science Conference and Workshop:"Crossing the Millennium: Integrating Spatial Technologies and Ecological Principles for a New Age in Fire Management," Boise, Idaho* (pp. 78-87).

Møller, J., & Waagepetersen, R. P. (2007). Modern statistics for spatial point processes*. *Scandinavian Journal of Statistics*, 34(4), 643-684.

Mueller, J., Loomis, J., & González-Cabán, A. (2009). Do repeated wildfires change homebuyers' demand for homes in high-risk areas? A hedonic analysis of the short and long-term effects of repeated wildfires on house prices in Southern California. *The Journal of Real Estate Finance and Economics*, 38(2), 155-172.

Ogata, Y. (1998). Space-time point-process models for earthquake occurrences. *Annals of the Institute of Statistical Mathematics*, 50(2), 379-402.

Ohlson, D. W., Berry, T. M., Gray, R. W., Blackwell, B. A., & Hawkes, B. C. (2006). Multi-attribute evaluation of landscape-level fuel management to reduce wildfire risk. *Forest Policy and Economics*, 8(8), 824-837.

Papangelou, F. (1974). The conditional intensity of general point processes and an application to line processes. *Probability Theory and Related Fields*, 28(3), 207-226.

Pastor, E., Zarate, L., Planas, E., & Arnaldos, J. (2003). Mathematical models and calculation systems for the study of wildland fire behaviour. *Progress in Energy and Combustion Science*, 29(2), 139-153.

Pearce, J. L., & Boyce, M. S. (2006). Modelling distribution and abundance with presence-only data. *Journal of Applied Ecology*, 43(3), 405-412.

Perry, G. L., Miller, B. P., & Enright, N. J. (2006). A comparison of methods for the statistical analysis of spatial point patterns in plant ecology. *Plant Ecology*, 187(1), 59-82.

Pew, K. L., & Larsen, C. P. S. (2001). GIS analysis of spatial and temporal patterns of human-caused wildfires in the temperate rain forest of Vancouver Island, Canada. *Forest ecology and management*, 140(1), 1-18

Picard, N., BAR-HEN, A. V. N. E. R., Mortier, F., & Chadoeuf, J. (2009). The multi-scale marked area-interaction point process: A model for the spatial pattern of trees. *Scandinavian journal of statistics*, 36(1), 23-41.

Podur, J., Martell, D. L., & Csillag, F. (2003). Spatial patterns of lightning-caused forest fires in Ontario, 1976–1998. *Ecological Modelling*, 164(1), 1-20.

Preisler, H. K., Brillinger, D. R., Burgan, R. E., & Benoit, J. W. (2004). Probability based models for estimation of wildfire risk. *International Journal of Wildland Fire*, 13(2), 133-142.

Prestemon, J. P., & Butry, D. T. (2005). Time to burn: modeling wildland arson as an auto-regressive crime function. *American journal of agricultural economics*, 87(3), 756-770.Prestemon, J. P., Hawbaker, T. J., Bowden, M., Carpenter, J., Brooks, M. T., Abt, K. L., ... & Scranton, S. (2013). Wildfire ignitions: A review of the science and recommendations for empirical modeling.

Prestemon, J. P., Pye, J. M., Butry, D. T., Holmes, T. P., & Mercer, D. E. (2002). Understanding broadscale wildfire risks in a human-dominated landscape. *Forest Science*, 48(4), 685-693.

R Development Core Team. (2010). R software.

Richards, G. D. (1990). An elliptical growth model of forest fire fronts and its numerical solution. *International Journal for Numerical Methods in Engineering*, 30(6), 1163-1179.

Ripley, B. D. (1977). Modelling spatial patterns. *Journal of the Royal Statistical Society B (Methodological)*, 172-212.

Ripley, B. D. (1991). *Statistical inference for spatial processes*. Cambridge university press.

Romero-Calcerrada, R., Novillo, C. J., Millington, J. D. A., & Gomez-Jimenez, I. (2008). GIS analysis of spatial patterns of human-caused wildfire ignition risk in the SW of Madrid (Central Spain). *Landscape Ecology*, 23(3), 341-354.

Rothermel, R. C. (1972). A mathematical model for predicting fire spread in wildland fuels.

Schmidt, D. A., Taylor, A. H., & Skinner, C. N. (2008). The influence of fuels treatment and landscape arrangement on simulated fire behavior, Southern Cascade range, California. *Forest Ecology and Management*, 255(8), 3170-3184.

Stein, A., & Georgiadis, N. (2006). Spatial marked point patterns for herd dispersion in a savanna wildlife herbivore community in Kenya. In *Case studies in spatial point process modeling* (pp. 261-273). Springer New York.

Stephens, S. L. (1998). Evaluation of the effects of silvicultural and fuels treatments on potential fire behaviour in Sierra Nevada mixed-conifer forests. *Forest Ecology and Management*, 105(1), 21-35.

Stoyan, D., & Penttinen, A. (2000). Recent applications of point process methods in forestry statistics. *Statistical Science*, 61-78.

Strauss, D. J. (1975). A model for clustering. *Biometrika*, 62(2), 467-475.

Sullivan, A. L. (2009a). Wildland surface fire spread modelling, 1990–2007. 1: Physical and quasi-physical models. *International Journal of Wildland Fire*, 18(4), 349-368.

Sullivan, A. L. (2009b). Wildland surface fire spread modelling, 1990–2007. 2: Empirical and quasi-empirical models. *International Journal of Wildland Fire*, 18(4), 369-386.

Sullivan, A. L. (2009c). Wildland surface fire spread modelling, 1990–2007. 3: Simulation and mathematical analogue models. *International Journal of Wildland Fire*, 18(4), 387-403.

Syphard, A. D., Radeloff, V. C., Keuler, N. S., Taylor, R. S., Hawbaker, T. J., Stewart, S. I., & Clayton, M. K. (2008). Predicting spatial patterns of fire on a southern California landscape. *International Journal of Wildland Fire*, 17(5), 602-613.

Thompson, M. P., & Calkin, D. E. (2011). Uncertainty and risk in wildland fire management: a review. *Journal of Environmental Management*, 92(8), 1895-1909.

Thompson, M. P., Calkin, D. E., Finney, M. A., Ager, A. A., & Gilbertson-Day, J. W. (2011). Integrated national-scale assessment of wildfire risk to human and ecological values. *Stochastic Environmental Research and Risk Assessment*, 25(6), 761-780.

Turner, R. (2009). Point patterns of forest fire locations. *Environmental and ecological statistics*, 16(2), 197-223.

Tutsch, M., Haider, W., Beardmore, B., Lertzman, K., Cooper, A. B., & Walker, R. C. (2010). Estimating the consequences of wildfire for wildfire risk assessment, a case study in the southern Gulf Islands, British Columbia, Canada. Canadian journal of forest research, 40(11), 2104-2114.

Tymstra, C. (2002). PROMETHEUS—the Canadian wildland fire growth model. *Initial Attack*, 2002, 8-9.

Uria-Diez, J., Ibáñez, R., & Mateu, J. (2013). Importance of habitat heterogeneity and biotic processes in the spatial distribution of a riparian herb (*Carex remota L.*): a point process approach. *Stochastic Environmental Research and Risk Assessment*, 27(1), 59-76.

Van Lieshout, M. N. M. (2000). *Markov point processes and their applications* (p. 41). London: Imperial College Press.

Vega-García, C., Woodard, P. M., & Lee, B. S. (1993). Geographic and temporal factors that seem to explain human-caused fire occurrence in Whitecourt Forest, Alberta. In *GIS'93 Symposium*.

Wallace, G. (1993). A numerical fire simulation-model. *International Journal of Wildland Fire*, 3(2), 111-116.

Warton, D. I., & Shepherd, L. C. (2010). Poisson point process models solve the "pseudo-absence problem" for presence-only data in ecology. *The Annals of Applied Statistics*, 4(3), 1383-1402.

Weber, R. O. (1989). Analytical models for fire spread due to radiation. *Combustion and flame*, 78(3), 398-408.

Weise, D. R., & Biging, G. S. (1997). A qualitative comparison of fire spread models incorporating wind and slope effects. *Forest Science*, 43(2), 170-180.

Yang, J., He, H.S., Shifley, S.R., & Gustafson, E.J. (2007). Spatial patterns of modern period human-caused fire occurrence in the Missouri Ozark highlands. *Forest Science*, 53(1), 1-15.